HAL
open science

Right temporoparietal junction underlies avoidance of moral transgression in Autism Spectrum Disorder

Y Hu, Am Pereira, X Gao, Bm Campos, Edmund A. Derrington, Brice Corgnet, X Zhou, F Cendes, Jean-Claude Dreher

To cite this version:

Y Hu, Am Pereira, X Gao, Bm Campos, Edmund A. Derrington, et al.. Right temporoparietal junction underlies avoidance of moral transgression in Autism Spectrum Disorder. Journal of Neuroscience, 2021, 41 (8), pp.1699-1715. 10.1523/jneurosci.1237-20.2020 . hal-02990821

HAL Id: hal-02990821

https://hal.science/hal-02990821v1

Submitted on 9 Nov 2020

HAL is a multi-disciplinary open access archive for the deposit and dissemination of scientific research documents, whether they are published or not. The documents may come from teaching and research institutions in France or abroad, or from public or private research centers.

L'archive ouverte pluridisciplinaire **HAL**, est destinée au dépôt et à la diffusion de documents scientifiques de niveau recherche, publiés ou non, émanant des établissements d'enseignement et de recherche français ou étrangers, des laboratoires publics ou privés.

JNeurosci Accepted Manuscript

JNeurosci
THE JOURNAL OF NEUROSCIENCE

Research Articles: Behavioral/Cognitive

Right temporoparietal junction underlies avoidance of moral transgression in Autism Spectrum Disorder

https://doi.org/10.1523/JNEUROSCI.1237-20.2020

Cite as: J. Neurosci 2020; 10.1523/JNEUROSCI.1237-20.2020

Received: 25 May 2020
Revised: 27 October 2020
Accepted: 28 October 2020

This Early Release article has been peer-reviewed and accepted, but has not been through the composition and copyediting processes. The final version may differ slightly in style or formatting and will contain links to any extended data.

Alerts: Sign up at www.jneurosci.org/alerts to receive customized email alerts when the fully formatted version of this article is published.

Copyright © 2020 the authors

JNeurosci Accepted Manuscript

Title: Right temporoparietal junction underlies avoidance of moral transgression in Autism Spectrum Disorder

Abbreviated title: Moral decisions and autism

Authors information:

Yang Hu[1,2,5†] , Alessandra M. Pereira[3†], Xiaoxue Gao[5],

Brunno M. Campos[3], Edmund Derrington[2,4], Brice Corgnet[7],

Xiaolin Zhou[1,5,6], Fernando Cendes[3], Jean-Claude Dreher[2,4*]

[1] Key Laboratory of Applied Brain and Cognitive Sciences, School of Business and Management, Shanghai International Studies University, 201620 Shanghai, China

[2] Laboratory of Neuroeconomics, Institut des Sciences Cognitives Marc Jeannerod, CNRS, 69675 Bron, France

[3] Neuroimaging Laboratory, School of Medical Sciences, The Brazilian Institute of Neuroscience and Neurotechnology, University of Campinas (UNICAMP), 13083-970 Campinas, Brazil

[4] Université Claude Bernard Lyon 1, 69100 Villeurbanne, France

[5] School of Psychological and Cognitive Sciences, Peking University, 100871 Beijing, China

[6] PKU-IDG/McGovern Institute for Brain Research, Peking University, 100871 Beijing, China

[7] EmLyon, 69130 Ecully, France

[*]Correspondence to: dreher@isc.cnrs.fr

[†]These authors equally contributed to this study.

Number of pages: 61

Number of figures: 10

Number of tables: 6

Number of words for abstract: 232

Number of words for introduction: 646

Number of words for discussion: 2,077

JNeurosci Accepted Manuscript

Competing interests: The authors declare no competing interests.

Acknowledgments: J-C.D. was funded by the IDEX-LYON from Université de Lyon (project INDEPTH) within the Programme Investissements d'Avenir (ANR-16-IDEX-0005) and of the LABEX CORTEX (ANR-11-LABX-0042) of Université de Lyon, within the program Investissements d'Avenir (ANR-11-IDEX-007) operated by the French National Research Agency, and grants from the Agence Nationale pour la Recherche and NSF in the CRCNS program (ANR n°16-NEUC-0003-01) and from Fondation de France (n°89590). F.C. was funded by São Paulo Research Foundation (FAPESP n°. 2013/07559-3) of Brazil. Y.H. was funded by China Postdoctoral Science Foundation (2019M660007). X.G. and X.Z. were supported by National Basic Research Program of China (973 Program: 2015CB856400) and National Natural Science Foundation of China (91232708, 31170972, 31630034, 71942001). X.G. was supported by China Postdoctoral Science Foundation (2019M650008) and National Natural Science Foundation of China (31900798). We thank the staff of the Imaging Center of the University of Campinas for helpful assistance with data collection for the fMRI study.

JNeurosci Accepted Manuscript

Abstract

Autism spectrum disorder (ASD) is characterized by a core deficit in theory-of-mind (ToM) ability, which extends to perturbations in moral judgment and decision-making. Although the function of the right temporoparietal junction (rTPJ), a key neural marker of ToM and morality, is known to be altered in autistic individuals, the neurocomputational mechanisms underlying its specific impairment in moral decision-making remain unclear. Here, we addressed this question by employing a novel fMRI task together with computational modeling and representational similarity analysis (RSA). ASD patients and healthy controls (HC) decided in public or private whether to incur a personal cost for funding a morally-good cause (Good Context) or receive a personal gain for benefiting a morally-bad cause (Bad Context). Compared with HC, individuals with ASD were much more likely to reject the opportunity to earn ill-gotten money by supporting a bad cause than HC. Computational modeling revealed that this resulted from unduly weighing benefits for themselves and the bad cause, suggesting that ASD patients apply a rule of refusing to serve a bad cause because they over-evaluate the negative consequences of their actions. Moreover, RSA revealed a reduced rTPJ representation of the information specific to moral contexts in ASD patients. Together, these findings indicate the contribution of rTPJ in representing information concerning moral rules and provide new insights for the neurobiological basis underpinning moral behaviors illustrated by a specific dysfunction of rTPJ in ASD patients.

Significance

Previous investigations have found an altered pattern of moral behaviors in individuals with autism spectrum disorder (ASD), closely associated with a dysfunction in the right temporoparietal junction (rTPJ). However, the specific neurocomputational mechanisms at play

JNeurosci Accepted Manuscript

that drive the dysfunction of the rTPJ in moral decision-making remain unclear. Here, we show that ASD individuals are more inflexible when following a moral rule even though an immoral action can benefit themselves, and suffer an undue concern about their ill-gotten gains and the moral cost. Moreover, a selectively reduced rTPJ representation of information concerning moral rules was observed in ASD patients. These findings deepen our understanding of the neurobiological roots that underlie atypical moral behaviors in ASD patients.

JNeurosci Accepted Manuscript

Introduction

Autism spectrum disorder (ASD) is a complex neurodevelopment disorder with evident impairments in social interaction, communication, and interpersonal relationships (APA, 2013), which are critically dependent on theory-of-mind (ToM) ability (Young et al., 2007; Margoni and Surian, 2016). These social deficits are also associated with atypical moral cognition. Indeed, individuals with ASD have difficulties in evaluating the moral appropriateness of actions in terms of the intentions of the protagonists in hypothetical scenarios (Moran et al., 2011; Buon et al., 2013; Fadda et al., 2016). ASD patients also conduct aberrant moral behaviors that lead to real consequences. For example, they are less sensitive to observation by others while making charitable decisions (Izuma et al., 2011).

Previous neuroimaging studies of healthy subjects lay a crucial foundation for improving our understanding of the neural basis underlying the atypical morality of ASD patients. One of the key regions is the right temporoparietal junction (rTPJ), which is not only the hub of ToM network (Schaafsma et al., 2014; Schurz et al., 2014), but is also well known for its crucial contribution to moral judgments (Young et al., 2007) and moral decisions involving trade-offs between self-interest and other's welfare (Morishima et al., 2012; Tusche et al., 2016). Importantly, prior fMRI studies have also shown an atypical rTPJ activation in ASD cohorts compared to healthy controls (HC) in a variety of social tasks that critically depend on ToM ability, such as processing naturalistic social situations (Pantelis et al., 2015), perceiving biological motion (Kana et al., 2009) or mentalizing about someone else (Lombardo et al., 2011). More relevantly, rTPJ in ASD patients was unable to display reliable neural patterns that distinguish intentional harm from accidental harm (Koster-Hale et al., 2013). While these studies provide direct evidence of a ToM-related dysfunction of rTPJ in ASD patients, the specific rTPJ dysfunction that drives atypical moral behaviors in ASD patients remains largely unknown.

JNeurosci Accepted Manuscript

To address this question, we employed a novel paradigm in an fMRI study where high-functioning ASD patients and HC decided whether to accept or reject a series of offers. In particular, we independently manipulated two factors, i.e., Audience (whether decisions were made in public or private) and Moral Context (whether the offer involves a trade-off between a personal financial loss and a charity donation, or between a personal financial gain and a donation to a morally bad cause). Moreover, the payoffs for participants and the associations varied across different trials in an orthogonal manner.

Combining computational modeling (Crockett, 2016; Konovalov et al., 2018) and multivariate-based representational similarity analyses (RSA) (Kriegeskorte et al., 2008), the present design allowed us to directly test two predictions about different aspects of atypical moral behaviors in ASD patients and their critical association with rTPJ dysfunction. The first prediction concerned social reputation (Frith and Frith, 2011), namely, how individuals care about their self-image in other's eyes. Evidence has shown that while making prosocial decisions, ASD patients show difficulties in sustaining a social reputation, which requires mentalizing ability (Izuma et al., 2011). Thus, compared with the HC group, ASD patients would show less distinction between their moral decisions made in public and in private. This would be associated with a reduced rTPJ engagement of representing information concerning social reputation, in presence or absence of an audience.

Our second hypothesis was inspired by studies of moral judgments that reveal autistic individuals tend to judge moral culpability more often in terms of consequences (Moran et al., 2011; Fadda et al., 2016; Salvano-Pardieu et al., 2016), and often over-evaluate the negative moral consequences (Moran et al., 2011; Bellesi et al., 2018). Hence, it was possible that compared to HC, ASD patients would display increased aversion to the consequences of an immoral action and therefore reject more offers that earn themselves morally-tainted profits. We

JNeurosci Accepted Manuscript

119 further explored whether such behavioral differences could be explained by a reduced rTPJ
120 representation of information concerning moral contexts in ASD patients.

JNeurosci Accepted Manuscript

Materials and Methods

Participants

A total of 48 participants were recruited for the present fMRI experiment. Specifically, 20 individuals with autism spectrum disorder (ASD; 4 females; 17.0 ± 3.0 years, ranging from 14 to 24 years; 3 left handedness) were recruited via those who attended psychiatric and pediatric neurology clinics as outpatients and fulfilled the inclusion criteria. 28 healthy controls (HC; 10 females; 18.9 ± 3.0 years, ranging from 14 to 25 years; 1 left handed) were recruited from the local community via fliers. Diagnoses of ASD were performed by a clinical pediatric neurologist according to the Autism Diagnostic Interview-revised (ADI-R; see **Table 1** for all clinical tests describing the two samples). There were no significant between-group differences in gender ($\chi(1)^2$ =1.395, p = 0.238) and IQ (total: t(43) = -1.795, p = 0.080; verbal: t(43) = -1.379, p = 0.175; execution: t(43) = -1.421, p = 0.162), except that ASD participants were slightly younger than HC participants (t(46) = -2.121, p = 0.039).

The study was performed at the Imaging Center of the University of Campinas and approved by the local ethics committee (plataformabrasil.saude.gov.br; reference number: CAAE 02388012.5.0000.5404; approved ethical statement: No. 1904090). All experimental protocols and procedures were conducted in accordance with the IRB guidelines for experimental testing and complied with the latest revision of the Declaration of Helsinki (BMJ 1991; 302: 1194).

Experimental Design and Task

We adopted a 2 × 2 within-subject design with a novel paradigm (also see Obeso et al., 2018; Qu et al., 2019). Specifically, participants decided whether to accept or reject a series of offers consisting of a personal profit or loss and a donation to a certain association, either in absence or presence of an audience (i.e., Audience: Private vs. Public; see Procedure for

JNeurosci Accepted Manuscript

details). In half of the trials, participants were confronted with offers involving a monetary loss for themselves but a financial gain to a local charity, "*The Child Hope Campaign*" (www.redeglobo.globo.com/criancaesperanca), which supports the education of children and adolescents in Brazil. In the other trials, participants considered offers that comprised a monetary gain for themselves but also a financial gain benefiting a morally-bad cause, "*No Dogs and Cats*" (www.naocaesegatos.net), which aims to clean the street by exterminating street animals. In other words, we manipulated moral contexts (i.e., Good vs. Bad) according to the cause involved in offers. In total, the present design yielded four experimental conditions, $\text{Public}_{\text{Good}}$, $\text{Public}_{\text{Bad}}$, $\text{Private}_{\text{Good}}$, and $\text{Private}_{\text{Bad}}$. Crucially, participants were informed that their decisions could have real consequences. Thus, if participants accepted the offer in the Good context, they would lose a certain amount of money and the charity would be paid. If they do so in the Bad context, they would earn the money and the bad cause would also be paid. However, if participants rejected the offer, neither they nor the involved association would gain or lose any money (see **Figure 1**). Participants were also informed that all trials (decisions) were independent from each other so that the incentive consequences would not accumulate across the experiment. Only one trial would be randomly selected and paid at the end of the experiment

One key aspect of the present design was that we varied the monetary stakes for the participants and the associations independently across trials within each condition. Personal payoffs (i.e., profits or losses) ranged from 1 to 8 in steps of 1 (unit: Brazillian Real; 1 Brazilian Real ≈ 0.2 USD). Donations to both associations ranged from 4 to 32 in the steps of 4. The personal payoff and the donation were orthogonal, which led to 64 different offers. Each offer appeared only once in each condition and thus summed up to 256 trials in total.

JNeurosci Accepted Manuscript

The functional scanning comprised four runs of 64 trials. Each moral context was assigned to either the first or the second of two runs. Each run consisted of two blocks, which included 32 trials presenting unique offers in either the Private or the Public condition. The order of runs involving Good/Bad moral contexts and Public/Private blocks were counterbalanced across participants. The trial order was randomized within each block. For each trial, participants were presented with the decision screen consisting of the payoff information for the participant (monetary gain or loss), and the association indicated by the corresponding symbol. The cue that signaled whether it was a Public (a picture of eyes) or a Private (i.e., a picture of a padlock) trial was also shown on the same screen. Here a cue of being watched was used as previous studies have consistently shown that it influences individuals' behaviors (Haley and Fessler, 2005; Izuma et al., 2008). Participants decided whether to accept or reject the offer by pressing the corresponding button on the button box with the right index or middle finger at their own pace. In the Private condition, once a response was made, the screen was unchanged for 0.5s to keep the chosen option private. In the Public condition, the chosen option was highlighted with a larger font, and the non-chosen option disappeared, which lasted slightly longer (1.5s) to further emphasize the presence of a witness (Qu et al., 2019). This was followed by a uniformly jittered fixation (2.5 – 6.5s), which ended the trial.

All visual stimuli were presented using Presentation v14 (Neurobehavioral Systems Inc., *Albany, CA, USA*) back-projected on a screen outside the scanner, using a mirror system attached to the head coil.

Procedure

On the day of scanning, participants (and their legal guardians when necessary) first signed the written informed consent and then were given the instructions. After that, they completed a series of comprehension questions to ensure that they fully understood the task. Importantly, they met with an independent audience and were informed that this person would

JNeurosci Accepted Manuscript

sit in the control room to witness their choices in some trials (i.e., in the Public condition) during the experiment. In the scanner, participants completed a practice session to get familiar with the paradigm and the response button. The scanning part consisted of four functional runs lasting around 35 min, which was followed by a 6-min structural scan. After that, participants indicated their liking for each association on an 11-point Likert scale (0 indicated “dislike very much”, 10 indicated “like very much”). Finally, participants were debriefed, paid, and thanked.

Data Acquisition

The imaging data were acquired on a 3-Tesla Philips Achieva MRI system with a 32-channel head coil (Best, *The Netherlands*) at the Imaging Center of University of Campinas. Functional data were acquired using T2*-weighted echo-planar imaging (EPI) sequences employing a BOLD contrast (TR = 2000 ms, TE = 30 ms; flip angle = 90°; slice thickness = 3 mm without gap, matrix = 80 × 80, FoV = 240 × 240 mm^2) in 40 axial slices. Slices were axially oriented along the AC-PC plane and acquired in an ascending order. A high-resolution structural T1-weighted image was also collected for every participant using a 3D MRI sequence (TR = 7 ms, TE = 3.2 ms; flip angle = 8°; slice thickness = 1 mm, matrix = 240 × 240, FoV = 240 × 240 mm^2).

Statistical Analyses

One ASD participant was excluded from behavioral analyses due to the invariant response pattern (i.e., rejecting all trials in the task). After checking the preprocessed fMRI data, we excluded two more HC participants (one because half of the scanning data was lost due to a technical reason, the other for excessive head motion [i.e., > 3 mm] in two out of four runs) and one more ASD participant (due to excessive head motion [i.e., > 5 mm] in three out of four

JNeurosci Accepted Manuscript

functional runs). Thus, 26 HC participants and 18 ASD participants were included for the fMRI analyses.

Behavioral Analyses

All behavioral analyses were conducted using R (http://www.r-project.org/) (R Core Team, 2014). All reported p values are two-tailed and $p < 0.05$ was considered statistically significant. Data visualization was performed via the "ggplot2" package (Wickham, 2016). We excluded trials with either extremely fast responses (i.e., < 200 ms) or extremely slow response (i.e., exceeding 3 SD of the individual mean decision time) from both the behavioral analyses and the model-based analyses. The percentage of trials excluded due to the criteria of decision time was 1.63% for the HC group and 1.89% for the ASD group.

For ease of interpretation, we defined the moral choices as those in which the participant accepted offers in the Good context or rejected offers in the Bad context. We performed the repeated mixed-effect logistic regression predicting the moral choice by the glmer function in "lme4" package (Bates et al., 2013), with Group (dummy variable; reference level: HC; same below), Audience (dummy variable; reference level: private; same below), Moral Context (dummy variable; reference level: good; same below), and their interactions (i.e., 3 two-way interactions and 1 three-way interaction) as the fixed-effect predictors. We also incorporated age as a covariate in the analyses to rule out its possible confounding effect. We included random-effect predictors that allowed varying intercepts across participants. For the statistical inference on each predictor, we performed the Type II Wald chi-square test on the model fits by using the Anova function in "car" package (Fox et al., 2016). Once the interactions were detected, we ran post-hoc regressions on the subset of data given the different groups and then

JNeurosci Accepted Manuscript

conditions. We reported the odds ratio (OR) as an index of effect size of each predictor on moral choices.

We also performed mixed-effect linear regression analyses on the log-transformed decision time (Anderson-Darling normality test: A = 431.33, $p < 0.001$) with the lmer function in "lme4" package, with the same fixed-effect predictors, random-effect predictors, and covariates as for the choice analyses. In addition, we also controlled the effect of specific decision (dummy variable; reference level: moral choice) in the regression model. We followed the procedure recommended by Luke (2017) to obtain the statistics for each predictor by applying the Satterthwaite approximations on the restricted maximum likelihood model (REML) fit via the "lmerTest" package (Luke, 2017). In addition, we reported the standardized coefficient (b_z) as an index of the effect size of each predictor on decision time together with other continuous dependent measures (e.g., rating, parameter estimates) using "EMAtools" (https://cran.r-project.org/web/packages/EMAtools/) and "lm.beta" package (https://cran.r-project.org/web/packages/lm.beta/) for mixed-effect and simple linear regression models respectively.

Computational Modeling

To examine how participants evaluated payoffs of each party and integrated them into a subjective value (SV), we compared the following 8 models with different utility functions characterizing participants' choices.

Model 1 was adapted from a recent study on moral decision making by Crockett *et al* (2014, 2015, 2017), which could be formally represented as follows:

$$\mathrm{SV}(M_S, M_O) = \begin{cases} -(\alpha - q * \theta) * M_S + (1 - \alpha + q * \theta) * M_O & if\ Good \\ (\alpha - q * \theta) * M_S - (1 - \alpha + q * \theta) * M_O & if\ Bad \end{cases}$$

JNeurosci Accepted Manuscript

where SV denotes the SV of the given trial if the participant chooses to accept. For rejection trials, SV is always 0 given the rule of the task (i.e., neither beneficiaries would gain the money; same for all models). Ms and Mo represent the payoff (gain or loss) for oneself and payoffs donated to the corresponding association. α (0 < α < 1) is the unknown parameter of social preference which arbitrates the relative weight on the payoff for the participant in the decision. θ (0 < θ < 1) is the unknown parameter characterizing the audience effect, which is modulated by an indicator function q (0 for private, 1 for public; same below). This model assumes that the subjective value was computed as a weighted summation of personal payoffs and payoffs donated to the association, and that people cared less about their own payoffs but increased the weights on the benefits donated to the association in public (vs. private). Model 2 was similar to Model 1 except that it adopted two separate α depending on the moral context in that trial.

Model 3 has a logic similar to Model 1, and was built upon studies adopting a donation task (Lopez-Persem et al., 2017; Qu et al., 2020):

$$\mathrm{SV}(M_S, M_O) = \begin{cases} -(\alpha - q * \theta) * M_S + (\beta + q * \theta) * M_O & if\ Good \\ (\alpha - q * \theta) * M_S + (\beta - q * \theta) * M_O & if\ Bad \end{cases}$$

where α and β are unknown parameters which capture the weight of the payoff for either the participant or the association involved in the trial (-20 < α, β < 20). Again, θ (0 < θ < 10) describes the audience effect which is represented by the indicator function q. Model 4 was similar to Model 3 except that it adopted two separate pairs of α and β according to the association involved in that trial (i.e., good cause or the bad cause).

Models 5-8 were established on the basis of the Fehr-Schmidt model (Fehr and Schmidt, 1999):

$$\mathrm{SV}(M_S, M_O) = \begin{cases} -M_S - \alpha * \max(M_O + M_S, 0) - \beta * \max(-M_S - M_O, 0) & if\ Good \\ M_S - \alpha * \max(M_O - M_S, 0) - \beta * \max(M_S - M_O, 0) & if\ Bad \end{cases}$$

JNeurosci Accepted Manuscript

where α and β measure the degree of aversion to payoff inequality in disadvantageous and advantageous situations respectively (i.e., how participants dislike that they themselves gained less/more than the association; 0 < α, β < 5). Among them, Model 5 adopted a fixed pair of α and β in all four conditions. Model 6 and Model 7 took different pairs of α and β either in terms of the audience or the moral context. Model 8 assumed that people showed distinct advantageous and disadvantageous inequality aversion that changed in each of the four conditions.

Given the softmax rule, we could estimate the probability of making a moral choice (i.e., accept in the Good context or reject in the Bad context) as below:

$$\mathrm{p}(SV_{moral}) = \frac{e^{\tau SV_{moral}}}{e^{\tau SV_{moral}} + e^{\tau SV_{immoral}}}$$

where τ refers to the inverse softmax temperature (0 < τ < 10) which denotes the sensitivity of individual's behavior to the difference in SV between moral and immoral choices.

We leveraged a Hierarchical Bayesian Analysis (HBA) approach (Gelman et al., 2014) to fit all the above candidate models via the "hBayesDM" package(Ahn et al., 2017). In general, HBA has several advantages over the traditional maximal likelihood estimation (MLE) approach such that it could provide more stable and accurate estimates, and estimate the posterior distribution of both the group-level and individual-level parameters simultaneously (Ahn et al., 2011). The "hBayesDM" package performs a full Bayesian inference and provides actual posterior distribution using a Markov Chain Monte Carlo (MCMC) sampling manner through the Stan language (Stan Development Team, 2016). Conforming to the default setting in this package, we assumed the individual-level parameters were drawn from a group-level normal distribution: *individual-level parameters ~ Normal* (μ, σ). We fit each candidate model with four

JNeurosci Accepted Manuscript

independent MCMC chains using 1,000 iterations after 2,000 iterations for the initial algorithm warmup per chain that results in 4,000 valid posterior samples. The convergence of the MCMC chains was assessed through Gelman-Rubin R-hat Statistics (Gelman and Rubin, 1992).

For model comparisons, we computed the leave-one-out information criterion (LOOIC) score for each candidate model (Bault et al., 2015). LOOIC score provides the estimate of out-of-sample predictive accuracy in a fully Bayesian way, which makes it more reliable than the point-estimate information criterion (e.g., AIC). By convention, the lower LOOIC score indicates better out-of-sample prediction accuracy of the candidate model. A difference score of 10 on the information criterion scale is considered decisive (Burnham and Anderson, 2004). We selected the model with the lowest LOOIC as the winning model for subsequent analysis of key parameters. A posterior predictive check was additionally implemented to examine the absolute performance of the winning model. In other words, we tested whether the prediction of the winning model could capture the actual behaviors. In terms of the actual trial-wise stimuli sequences, we employed each individual's joint posterior MCMC samples (i.e., 4,000 times) to generate new choice datasets correspondingly (i.e., 4,000 choices per trial per participant). Then we calculated the mean proportion of moral choices of each experimental condition in these new datasets for each subject, respectively. We performed *Pearson* correlation to examine to what degree the predicted proportion of moral choice correlated with the actual proportion across individuals in each condition, respectively.

fMRI Data Preprocessing

Functional imaging data were analyzed using SPM12 (Wellcome Trust Centre for Neuroimaging, University College London, *London, UK*). The preprocessing procedure followed the pipeline recommended by SPM12. In particular, functional images (EPI) were first realigned

JNeurosci Accepted Manuscript

to the first volume to correct motion artifacts, unwarped, and corrected for slice timing. Next, the structural T_1 image was segmented into white-matter, grey-matter and cerebrospinal fluid with the skull removed, and co-registered to the mean functional images. Then all functional images were normalized to the MNI space, resampled with a $2 \times 2 \times 2$ mm^3 resolution, in terms of parameters generated in the previous step. Last, the normalized functional images were smoothed using an 8-mm isotropic full width half maximum (FWHM) based on a Gaussian kernel.

Within-Subject Representational Similarity Analyses (RSA)

To clarify what information rTPJ exactly represents during the decision period that distinguished ASD patients from HC participants, we carried out a within-subject RSA in Python 3.6.8 using the *nltools* package (version 0.3.14; https://github.com/cosanlab/nltools). Some preparation was performed before implementing RSA. In particular, we established a trial-wise general linear model (GLM) for each participant, which included the onsets of the decision screen with the duration of decision time of each valid trial. Here, valid trials were those that conformed to neither the exclusion criterion for the behavioral data (trials with extremely fast or slow responses; see above for details) nor the fMRI data (trials in runs with excessive head motion). The onsets of button press and invalid trials were also modeled as separate regressors of no interest. In addition, six movement parameters were added to this GLM as covariates to account for artifacts of head motion. The canonical hemodynamic response function (HRF) was used and a high-pass temporal filtering was performed with a default cut-off value of 128s to remove low-frequency drifts. After the parameter estimation, we built up the trial-wise contrasts which were used for subsequent RSA.

JNeurosci Accepted Manuscript

Our analyses concentrated on rTPJ given our hypotheses. Notably, we took two different ways to define the cluster of rTPJ to circumvent the potential effect of ROI selection on results. These included defining it via a whole-brain parcellation based on meta-analytic functional coactivation of the Neurosynth database (i.e., the parcellation-based ROI; https://neurovault.org/collections/2099/; including a total of 1,750 voxels, with a volume of 2×2×2 mm^3 per voxel, same below) or via a coordinate-based manner given a recent meta-analysis on neural correlates of ToM (Schurz et al., 2014) (i.e., the coordinate-based ROI; a sphere with a radius of 10mm centering on the MNI coordinates of 56/-56/18; 515 voxels in total).

We first extracted the parameter estimates (i.e., contrast value in arbitrary units) of rTPJ from these 1st-level contrast images of valid trials for each participant respectively. Next, we constructed the individual-level neural representation distance matrix (RDM) by computing the pairwise correlation dissimilarity of activation patterns within this mask between each pair of valid trials. We also built up the same neural RDM for lTPJ as a control region (i.e., the parcellation-based ROI: 1,626 voxels in total; the coordinate-based ROI (Schurz et al., 2014), a sphere with a radius of 10mm centering on the MNI coordinates of -53/-59/20; 515 voxels in total). In line with our research goal, we constructed two main cognitive RDMs in light of the trial-wise information of reputation (i.e., arbitrary code: 0 = Private, 1 = Public), and Moral Context (i.e., 0 = Bad, 1 = Good) by calculating the Euclidean distance between each pair of trials. We also built up two additional cognitive RDMs using the trial-wise information of payoffs for the participant (i.e., from 1 to 8 in step of 1), and payoffs for associations (i.e., from 4 to 32 in step of 4) as controls. These cognitive RDMs measured the dissimilarity between trials given corresponding information. Notably, we sorted all trials according to the order of Audience, Moral Context, payoff for the participant, and payoff for associations (the charity or the bad cause) to guarantee the information contained by both the neural and cognitive RDMs was

JNeurosci Accepted Manuscript

matched with each other. To make these cognitive RDMs comparable, we rescaled them within the range from 0 (i.e., the most similar) to 1 (i.e., the most dissimilar). Then we performed Spearman's rank-order correlation between the neural RDM and the cognitive RDM for each participant.

For the group-level statistical tests, we first implemented the Fisher r-to-z transformation on the Spearman's rho, and then performed the permutation-based two-sample t-test (i.e., the number of permutations: 5,000) on these statistics between the two groups for each cognitive RDM separately. To further examine the robustness of these findings, we applied the above analyses using all 256 trials. To this end, a new GLM was established that modeled the onset of the decision screen of all trials to further construct the neural RDM. The remaining details and procedures were the same as mentioned above.

Supplementary Univariate Analyses

We also performed a traditional univariate GLM analysis to examine whether the mean neural activations were modulated by different conditions and how neural signals in ASD patients differed from healthy controls, focusing on the rTPJ. At the individual level, we incorporated the onsets of the decision phase of all conditions (i.e., $\text{Private}_{\text{Good}}$, $\text{Private}_{\text{Bad}}$, $\text{Public}_{\text{Good}}$, $\text{Public}_{\text{Bad}}$) in valid trials as regressors of interest. Similarly, the onsets of button press together with invalid trials as well as head motion parameters were also modelled as separate regressors of no interest. After the parameter estimation, we constructed the following contrasts concerning the main effect of Audience (i.e., Public - Private) and Moral Context (i.e., Good - Bad). These contrast images were fed to the group-level one-sample T-test for within-group analyses or independent two-sample T-tests for between-group analyses. Given the goal of this analysis, we performed a small volume correction (SVC) within the rTPJ mask. To match the multivariate analyses, we adopted two independent rTPJ masks from different sources (i.e., the parcellation-based ROI and the coordinate-based ROI; see above for details). For the

JNeurosci Accepted Manuscript

403 completeness of the analyses, we also performed the same analyses using the ITPJ mask.
404 Otherwise, we adopted a whole-brain threshold of $p < 0.001$ uncorrected at the voxel-level
405 together with $p < 0.05$ FWE corrected at the cluster-level (Eklund et al., 2016).

JNeurosci Accepted Manuscript

Results

Subjective evaluation on associations

Post-task rating on a 0-10 Likert scale (0 indicates “do not like the association at all”, 10 indicates “like the association very much”) revealed that both ASD patients and healthy controls favored the charity (ASD vs. healthy controls: 9.3 ± 1.4 vs. 8.8 ± 1.2) and disliked the bad cause (0.0 ± 0.0 vs. 0.3 ± 0.6). No between-group difference was observed in the subjective rating for the charity (b = 0.43, SE = 0.39, t(44) = 1.11, p = 0.274, b_z = 0.17) and bad cause (b = -0.22, SE = 0.14, t(44) = -1.56, p = 0.125, b_z = -0.23).

ASD patients not only fail to consider social reputation but also rigorously conform to a rule in curbing their immoral behaviors

Mixed-effect logistic regressions revealed that participants were more likely to behave morally in the Bad than the Good context (i.e., rejecting more frequently the offer in the Bad context than accepting it in the Good context; a main effect of Moral Context: $\chi^2(1) = 632.68$, $p < 0.001$). More importantly, significant interaction effects were identified between Group and Audience ($\chi^2(1) = 4.50$, $p = 0.034$) as well as between Group and Moral Context ($\chi^2(1) = 59.33$, $p < 0.001$) on choosing the moral option (i.e., accepting the offer to benefit a charity or rejecting the offer to benefit a morally-bad cause; see **Figure 2**). No other main effect (*ps* > 0.09) or interaction effect was detected (*ps* > 0.57).

To understand the first interaction effect, we performed *post-hoc* analyses on the dataset of the ASD and the HC groups, respectively. For each analysis, we ran a similar logistic regression, including the main effect of audience and context as the fixed-effect predictors. The Audience × Moral Context interaction was dropped from these analyses as neither this effect ($\chi^2(1) = 0.31$, $p = 0.580$) nor the three-way interaction effect ($\chi^2(1) = 0.30$, $p = 0.586$) was

JNeurosci Accepted Manuscript

significant in the main analysis. The results showed that while healthy controls were more likely to make the moral choice when they were observed in the Public condition (vs. Private; OR = 1.16, b = 0.15, SE = 0.06, p = 0.012), ASD patients did not change their behaviors significantly depending on the presence or absence of a witness (OR = 0.93, b = -0.08, SE = 0.08, p = 0.371).

To understand the second interaction effect, we performed similar regression analyses using trials in the Good and Bad context separately. For each *post-hoc* regression analysis, we incorporated Group and Audience, along with their interaction as the fixed-effect predictors while controlling for the effect of the payoff for participants and associations in these analyses (same below for analyses on decision time). We only observed a strong main effect of Group ($\chi^2(1) = 5.05$, p = 0.025) and a Group × Audience interaction effect in the Bad context ($\chi^2(1) = 4.04$, p = 0.044), which was mainly driven by a drastically enhanced probability of behaving morally in the ASD group (vs. HC) when deciding privately (OR = 64.25, b = 4.16, SE = 1.53, p = 0.006). Neither of these effects was significant in the Good context (ps > 0.12; see **Table 2** for details of regression outputs).

ASD patients over-evaluate the immoral gains for both themselves and the bad cause

We developed 8 models with different utility functions characterizing participants' choices in ASD and HC groups separately. Model estimation and comparison was performed with a Hierarchical Bayesian Analysis (HBA) approach (Gelman et al., 2014) via the "hBayesDM" package (see Methods for details). R-hat values of all estimated parameters of all models are close to 1.0 (i.e., smaller than 1.06 in the worst case), which showed sufficient convergence of the MCMC chains (Gelman and Rubin, 1992). Hierarchical Bayesian model comparison showed that model 4 (see below for the utility function) has the lowest leave-one-out information criterion

JNeurosci Accepted Manuscript

(LOOIC) scores, indicating that it fits to the current dataset the best compared with other competitive models (see **Figure 3A**).

$$\mathrm{SV}(M_S, M_O) = \begin{cases} -(\alpha_{Good} - q * \theta) * M_S + (\beta_{Good} + q * \theta) * M_O & if\ Good \\ (\alpha_{Bad} - q * \theta) * M_S + (\beta_{Bad} - q * \theta) * M_O & if\ Bad \end{cases}$$

Here, SV denotes the subjective value of the given trial depending on the specific choice made by the participant. Ms and Mo represent the payoff (gain or loss) for oneself and each association respectively. Established on the basis of a donation task (Lopez-Persem et al., 2017), the winning model assumed that people weighed their own payoff (measured by α: α_{good}, α_{bad}) and the benefits for associations (measured by β: β_{good}, β_{bad}) separately given the moral contexts involved in the decisions. θ measured the audience effect, which was modulated by an indicator function q (0 for private, 1 for public; see Methods for details). Posterior predictive check further confirmed that the simulated choice behaviors in light of the parameter estimates of the winning model can nicely capture the actual behaviors by showing a high correlation between each other (i.e., for both HC and ASD group: Pearson's rs > 0.99, *ps* < 0.001; see **Figure 3B**).

Next, we examined how parameters derived from the winning model vary in terms of groups and experimental conditions. To this end, we extracted the individual-level posterior mean of key parameters (i.e., α, β, and θ) and performed linear regression, including Group as the predictor on each of them, respectively. To test the Group × Association interaction on α and β, we regressed groups on the difference score between two contexts for each of the parameters. For all these regression analyses, we also added age as a covariate to control for its confounding effect.

We first showed a significant group × association interaction on both α (b = 7.93, SE = 3.91, t(44) = 2.03, *p* = 0.049; b_z = 0.30) and β (b = -10.88, SE = 3.46, t(44) = -3.14, *p* = 0.003; b_z = -0.43). Simple-effect analyses showed a significant decrease of decision weights on payoffs,

JNeurosci Accepted Manuscript

in ASD patients, for both themselves (α_{HC} vs. α_{ASD}: 0.90 ± 11.74 vs. -9.27 ± 10.13, t(44) = -3.14, p = 0.003; b_z = -0.45) and the morally-bad cause (β_{HC} vs. β_{ASD}: -4.87 ± 5.02 vs. -11.52 ± 8.67, t(44) = -2.96, p = 0.005; b_z = -0.41). No between-group difference was observed in either parameter when participants weighed the trade-off between personal financial losses (α_{HC} vs. α_{ASD}: 11.18 ± 6.41 vs. 8.89 ± 9.09, t(44) = -1.26, p = 0.216; b_z = -0.19) and the donation to a charity (β_{HC} vs. β_{ASD}: 4.38 ± 4.04 vs. 6.78 ± 7.83, t(44) = 1.56, p = 0.126; b_z = 0.24; see **Figure 4A**). Notably, the correlation between α and β was not significant across moral contexts in either group (ASD group: Good context: r = -0.177, p = 0.469; Bad context: r = -0.242, p = 0.319; HC group: Good context: r = -0.018, p = 0.928; Bad context: r = -0.003, p = 0.989; see **Figure 4B**). This indicates that participants value payoffs for oneself and the causes (associations) independently. Consistent with the behavioral finding, we also observed a trend-to-significance for the between-group difference in θ, namely, that ASD patients exhibited a reduced audience effect compared to HC participants during moral decision-making (θ_{HC} vs. θ_{ASD}: 0.39 ± 0.67 vs. 0.17 ± 0.12, t(44) = -1.80, p = 0.080, b_z = -0.27).

ASD patients do not differ from HC in decision time in either moral context

Mixed-effect linear regression on log-transformed decision time showed a significant three-way interaction between Group, Audience, and Moral Context (F(1,11769) = 6.02, p = 0.014), along with a Group × Moral Context interaction effect (F(1,11769) = 100.20, p < 0.001) and a main effect of Moral Context (F(1,11772) = 299.76, p < 0.001) after controlling for the effect of specific choices (F(1,11804) = 3.76, p = 0.052; see **Figure 5**). Splitting the dataset according to Moral Context, *post-hoc* analyses revealed a significant Group × Audience interaction effect when participants decided whether to serve a good cause at a personal cost (F(1,5860) = 4.28, p = 0.039) and a trend-to-significant interaction effect in the Bad context (F(1,5859) = 3.76, p = 0.053). However, neither the main effect of Group in the Good (ASD:

JNeurosci Accepted Manuscript

1676.5 ± 527.7 ms; HC: 1490.0 ± 399.5 ms; F(1,44) = 0.51, p = 0.479) nor the Bad context (ASD: 1525.7 ± 828.1 ms; HC: 1445.5 ± 500.9 ms; F(1,44) = 0.17, p = 0.682) was significant. The interaction effect in the Good context was driven by a slightly larger difference in decision time between groups when they made decisions in public (ASD: 1709.5 ± 558.8 ms; HC: 1467.9 ± 379.3 ms) as compared to private (ASD: 1645.5 ± 526.0 ms; HC: 1514.1 ± 448.9 ms). However, neither of these between-group differences was statistically significant (public: b = 0.09, SE = 0.09, t(44) = 0.98, p = 0.334, b_z = 0.29; private: b = 0.04, SE = 0.10, t(44) = 0.42, p = 0.678, b_z = 0.13; see **Table 3** for details of regression output).

Imaging Results

Decreased neural representation of moral contexts in the rTPJ of ASD patients

To examine how the decision-related neural patterns differ in representing information contributing to the value computation and final decisions between ASD patients and HC participants, we performed a within-subject RSA (see **Figure 6** for the illustration of RSA procedure). Given our hypotheses, we focused our analysis on the rTPJ. To avoid bias on results caused by ROI selection to the maximum degree, we defined the rTPJ in two different ways, either via a whole-brain parcellation based on meta-analytic functional coactivation of the Neurosynth database (i.e., the Parcellation-Based ROI) or via a coordinate-based manner given a recent meta-analysis on neural correlates of ToM (Schurz et al., 2014) (i.e., the Coordinate-Based ROI; see Methods for details).

Regardless of the ROI approach, we consistently found that compared with HC group, ASD patients only showed a reduced representation of the information of the identity of associations in the rTPJ (ASD vs. HC: the Parcellation-Based ROI: Spearman's rho = 0.101 ± 0.047 vs. 0.150 ± 0.071; $p_{permutation}$ = 0.013; the Coordinate-Based ROI: 0.066 ± 0.036 vs. 0.119

JNeurosci Accepted Manuscript

± 0.070; $p_{permutation}$ = 0.006). These significant differences held after ruling out the confounding effect of age. Importantly, such a between-group difference of similarity was not observed between the neural RDM in the rTPJ and other cognitive RDMs (the Parcellation-Based ROI: $ps_{permutation}$ > 0.20; the Coordinate-Based ROI: $ps_{permutation}$ > 0.38) or between the neural RDM in the left TPJ and all the cognitive RDMs (the Parcellation-Based ROI: $ps_{permutation}$ > 0.17; the Coordinate-Based ROI: $ps_{permutation}$ > 0.30; see **Figure 7**; also see **Table 4** for details). *Post-hoc* 2 (group) × 4 (cognitive RDM) mixed ANOVA on the Fisher r-to-z transformed Spearman's rho revealed a strong interaction between group and cognitive RDM only in rTPJ (the Parcellation-Based ROI: F(3,126) = 6.09, p < 0.001; the Coordinate-Based ROI: F(3,126) = 8.37, p < 0.001) but not in lTPJ (the Parcellation-Based ROI: F(3,126) = 0.65, p = 0.585; the Coordinate-Based ROI: F(3,126) = 0.42, p = 0.743) after controlling for the age difference, which further confirmed that the reduced ability to represent the information of moral context in ASD patients was uniquely reflected in rTPJ. Finally, to further examine the robustness of the above findings, we also applied the above analyses using all 256 trials, which did not affect the results (see **Figure 8**; also see **Table 5** for details).

Univariate Results in rTPJ

We first investigated whether the neural audience effect in rTPJ (i.e., Public > Private) in healthy controls reported in Qu et al. (2019) could be replicated in the present study. The results showed that the rTPJ activity was not significantly higher in the Public (vs. Private) condition (no voxel survived under a threshold of p < 0.005 uncorrected at the voxel-level with k = 10, in either rTPJ mask; see **Figure 9A**). One possibility could be that the neural audience effect of rTPJ was modulated by large individual differences in the behavioral audience effect across individuals, which blurred the main effect. To test this possibility, we extracted the mean activity (contrast value) of the rTPJ from each condition, and then computed a neural index of

JNeurosci Accepted Manuscript

audience effect for each individual (i.e., 0.5*[($Public_{Good}$ + $Public_{Bad}$) - ($Private_{Good}$ + $Private_{Bad}$)]). We also defined a behavioral index of audience effect on the proportion of moral choice, which was calculated with the same equation. Results showed that the *Pearson* correlation between these two indices was not significant (the parcellation-based ROI: $r(24) = 0.02$, $p = 0.914$; the coordinate-based ROI: $r(24) = -0.06$, $p = 0.761$; see **Figure 9B**). Furthermore, the between-group comparison did not reveal a significant result in the audience effect in rTPJ (i.e., no voxel survived under the threshold mentioned above; see **Figure 10**). Besides, no significant difference in the neural activity was observed in the rTPJ between the Good and Bad context in the HC group or between two groups (i.e., no voxel survived under the threshold mentioned above). For the completeness of the analyses, we also applied the same analyses to lTPJ, yielding similar results (see **Figure 9 and 10**; also see **Table 6** for the whole-brain results under a liberal threshold).

JNeurosci Accepted Manuscript

Discussion

When facing moral dilemmas such as earning ill-gotten money by supporting a bad cause, or donating to a charity at a personal cost, how do autistic individuals choose? Do they vary their (im)moral behaviors with respect to the presence or absence of someone else, or contingent on moral concerns elicited by specific contexts (i.e., serving a good or a bad cause)? What neurocomputational mechanisms underlie such behavioral changes? In the present model-based fMRI study, we attempted to answer these questions by adopting a novel task in which individuals decided among trade-offs between personal benefits/losses and context-sensitive moral concerns while also, perhaps, considering their social reputation. Our behavioral results reveal that the moral behavior of ASD patients differs from healthy controls in two aspects.

First, ASD patients, unlike healthy controls, blurred the distinction between private and public conditions while making moral decisions. This finding not only coheres with the ToM deficit hypothesis of ASD patients (Baron-Cohen et al., 1985; Baron-Cohen, 2001) but also agrees with previous findings using a trade-off between suffering personal losses and donating to a good cause (Izuma et al., 2011). Moreover, it extends the unawareness of social reputation in autism to include an immoral context where individuals are confronted with a moral conflict between personal profits and a cost brought by benefiting an immoral cause. This first finding confirms that ASD patients seem unable to take into account their social reputation while making (im)moral choices consistently across contexts (Izuma et al., 2011).

Second, a robust behavioral difference between ASD patients and healthy controls was found in specifically one moral context. ASD patients generally refused more offers in the Bad context that could have earned extra money for themselves but which resulted in an immoral consequence. No similar between-group difference was observed in the Good context. Note

JNeurosci Accepted Manuscript

that decision difficulty cannot explain these behavioral effects because no decision time difference was observed between the two groups. Furthermore, this effect cannot be attributed to their greater (dis)like for the morally-bad cause because there was no significant between-group difference on subjective ratings.

Our computational modeling approach provides crucial insights to understand further this difference in ASD patients, which is specific to moral behaviors serving a bad cause. In parallel to the choice findings, ASD patients drastically lowered their decision weights on payoffs that would be earned both for themselves and the morally-bad cause, whereas they valued the personal losses and the charity's benefits similarly to healthy controls. These findings strongly indicate an atypical valuation of morally-tainted personal profits and moral costs brought by benefiting a bad cause in autistic individuals. This probably lead to their extremely high rejection rate for immoral offers. Our results fit the literature on moral judgment, which has shown that ASD patients exhibit an excessive valuation of negative consequences when judging the moral appropriateness or permissibility of actions. For example, Moran and colleagues (2011) reported that ASD participants considered accidental negative outcomes less permissible than healthy controls, whereas both groups rated other types of events as having similar moral appropriateness. In a more recent study, a similar effect was observed; namely, ASD patients judged a protagonist's immoral but understandable action (e.g., a husband stealing medicine sold at an unaffordable price to save his fatally sick wife) as less morally acceptable than healthy controls did (Schaller et al., 2019). In agreement with these findings, our results suggest that autistic individuals may apply a rule of refusing to serve an immoral cause because they over-evaluate the negative consequences of their actions. This might result in insensitivity in ASD patients who have difficulty in adjusting their behaviors regarding their personal interests that might be associated with immoral consequences.

JNeurosci Accepted Manuscript

Another possible explanatory factor of ASD participants' tendency to make overly-moral decisions in the Bad context is behavioral rigidity, a core symptom for clinical diagnosis of ASD (APA, 2013). Previous studies have revealed that compared with healthy controls, individuals with ASD were more likely to show repetitive behaviors in a variety of cognitive tasks (D'Cruz et al., 2013; Watanabe et al., 2019). Hence, it is possible that behavioral rigidity, at least to some extent, is a more general mechanism that contributes to the overly-moral behaviors in the Bad context (i.e., rejecting over 85% of the trials). Nonetheless, this explanation should be treated with caution because it seems not to account well for the behaviors of ASD patients in the Good context, where they behaved in a comparatively more flexible fashion (i.e., accepting around 60% of the trials).

At the brain level, we performed within-subject RSA to examine how different types of information (social reputation, moral contexts, payoffs for each party), that contribute to the final decision, were represented in the rTPJ, and how distinct rTPJ representations distinguish ASD patients from healthy controls. Compared with the traditional univariate approach, RSA takes advantage of neural patterns from multiple voxels, and proves to be more sensitive to subtle experimental effects that might be masked by the averaged local neural responses (Norman et al., 2006; Hebart and Baker, 2018). RSA is also considered to be more informative, because it takes into account the variability within multi-voxel patterns (Kriegeskorte et al., 2008; Popal et al., 2020). We observed a reduced association (representation similarity) in ASD patients (vs. healthy controls) between the trial-by-trial multivariate rTPJ patterns and the information structure unique to the moral contexts, despite that, such a representation in rTPJ is present in both groups. The representations of other types of information (i.e., social reputation and payoffs for each party) did not differ between groups. Together with a much higher rejection rate, as well as atypical weights on payoffs in the bad context, this RSA finding provides a neural account for previous findings that autistic individuals are inclined to judge moral culpability more

JNeurosci Accepted Manuscript

severely than HC on the basis of its consequences. This distinguishes ASD patients from HC, who prioritize intentions to guide their moral judgments (Fadda et al., 2016; Salvano-Pardieu et al., 2016; Bellesi et al., 2018). Notably, our results showed the group-difference in representational similarity was only detected in rTPJ but not in lTPJ, further indicating a unique role of rTPJ in specifically representing information concerning moral contexts.

Regarding the rTPJ's function, our RSA finding is consistent with a recent TMS study in healthy volunteers that revealed a context-sensitive moral role of rTPJ in signaling moral conflicts between personal benefits and moral values (Obeso et al., 2018). That study evidenced an asymmetrical TMS effect of rTPJ on moral behaviors depending on the moral context. Specifically, healthy participants under rTPJ stimulation were more altruistic such that they accepted more offers of donating to a charity at a personal cost regardless of donation amounts, whereas rTPJ disruption inhibited participants from accepting offers to earn morally-tainted money only when benefits to the bad cause were large. Building upon this finding, the present study provides further evidence using a different approach to reveal that rTPJ is critically involved in representing the moral contexts that flexibly modulate the trade-off between personal benefits and other's welfare during decision-making, which extends our understanding of the rTPJ function.

Notably, our univariate fMRI results did not reveal a neural audience effect in rTPJ in the healthy controls as was initially expected. Although previous studies provided evidence (Izuma, 2012; Qu et al., 2019) suggesting that TPJ is involved in social reputation, negative evidence also exists. For instance, a recent transcranial magnetic stimulation (TMS) study using a similar experimental paradigm has shown that disrupting rTPJ (vs. sham) does not influence the audience effect on moral decisions in healthy individuals (Obeso et al., 2018). In addition, two earlier fMRI studies failed to find an increased activation of rTPJ in response to the presence (vs. absence) of observers while healthy participants made charitable decisions (Izuma et al., 2010b)

JNeurosci Accepted Manuscript

660 or social evaluation (Izuma et al., 2010a). However, it is also worth noting that non-significant
661 results do not necessarily reflect a true null effect (Makin and Xivry, 2019). Also, our RSA result
662 suggests that multi-voxel patterns of rTPJ represent the information of social reputation in
663 healthy controls. Further studies are needed to clarify whether and how rTPJ plays a role in
664 reputation-based decision-making.

665 Intriguingly, we did not observe a between-group difference of rTPJ in representing
666 information about social reputation, although, as expected, a small-but-significant effect of social
667 reputation on moral behaviors was observed only in healthy controls rather than ASD patients.
668 At first glance, this finding may seem at odds with the well-established role of the rTPJ in
669 mentalizing (and relevant social abilities) in both healthy participants (Hampton et al., 2008;
670 Young et al., 2010; Carter et al., 2012; Morishima et al., 2012; Schurz et al., 2014; Hutcherson
671 et al., 2015; Strombach et al., 2015; Hill et al., 2017; Hu et al., 2018; Qu et al., 2019) and ASD
672 populations (Kana et al., 2009; Lombardo et al., 2011; Koster-Hale et al., 2013). These previous
673 findings indicate that the deficiency of ToM ability, reflected by the dysfunction of rTPJ,
674 determines the anomaly in moral behaviors in autistic cohorts. However, it should be noted that
675 evidence also exists, revealing that ASD patients may preserve some degree of ToM ability to
676 guide their intent-based moral judgments. For instance, one study showed that autistic adults
677 not only exhibit performance comparable to healthy controls in a false belief task but also report
678 similar moral permissibility when judging intended harms with neutral outcomes (Moran et al.,
679 2011). Another study even reported an increased sensitivity to intention during moral judgment
680 in Asperger syndrome compared with healthy controls (Channon et al., 2011). Consistent with
681 these studies, our RSA results also suggest that the ability to represent the information of social
682 reputation in rTPJ is partially intact in ASD patients. These findings indicate that the ability to
683 infer and base moral judgments on intentionality may be still present in ASD individuals, and
684 potentially explains why we did not observe a between-group difference of rTPJ in representing

JNeurosci Accepted Manuscript

social reputation in our task. It has also been proposed that the method of inferring intentionality differs between autistic and neurotypical participants (Dempsey et al., 2019). Here, a reduced rTPJ representation similarity in ASD, unique to the moral context, explains that patients excessively consider the negative consequences of an immoral action. This may block further recruitment of the intent-based system and thus lead to a failure to consider social reputation when making choices. Future studies may consider adopting tasks that involve both moral judgment and decision-making and implement non-invasive brain stimulation methods to target the rTPJ of ASD patients to provide causal evidence for this possibility.

Despite the strengths of this study, there are two potential limitations. First, the sample size is relatively small for the ASD group, which could have lowered the statistical power for the fMRI data analyses. Second, our sample has a relatively wide age range that covers the transition period from adolescence to early adulthood, during which time changes in sociocognitive processes and moral cognition continue to occur (Eisenberg and Morris, 2004; Blakemore and Mills, 2014; Kilford et al., 2016). Evidence indicates that mentalizing ability is still undergoing development in late adolescence (Dumontheil et al., 2010). More relevantly, previous studies have shown a distinct pattern in adolescents (vs. adults) for prosocial behaviors (Padilla-Walker et al., 2018) or the susceptibility to the audience effect (Wolf et al., 2015). Importantly, these changes are considered to be crucially associated with the development of the social brain network in adolescence (Blakemore, 2008; Kilford et al., 2016). Taking TPJ as an example, evidence from brain imaging studies showed that both structural and functional features of this region vary during this transition period (Blakemore et al., 2007; Mills et al., 2014). Hence, the age-related heterogeneity of our sample may have had some impact on our results, although we controlled for age-related differences in our between-group analyses. Future studies with a larger sample or less age heterogeneity would allow more definite conclusions.

JNeurosci Accepted Manuscript

To conclude, the present study, combining computational modeling with multivariate fMRI analyses, uncovers the neurocomputational changes of the rTPJ during moral behaviors in autistic individuals. They are characterized not only by a failure to consider social reputation but also, more predominantly, by an over-sensitivity to the negative consequences caused by immoral actions. This difference in moral cognition and behaviors in ASD patients is specifically associated with rTPJ, and consists of a reduced capability to represent information concerning moral contexts. Our findings provide novel insights for a better understanding of the neurobiological basis underlying atypical moral behaviors in ASD patients.

JNeurosci Accepted Manuscript

References

Ahn W-Y, Haines N, Zhang L (2017) Revealing neuro-computational mechanisms of reinforcement learning and decision-making with the hBayesDM package. Computational Psychiatry 1:24-57.

Ahn W-Y, Krawitz A, Kim W, Busemeyer JR, Brown JW (2011) A model-based fMRI analysis with hierarchical Bayesian parameter estimation. Journal of neuroscience, psychology, and economics 4:95.

APA (2013) Diagnostic and statistical manual of mental disorders: DSM-5 (5th ed.).

Baron-Cohen S (2001) Theory of mind and autism: A review. International review of research in mental retardation 23:169-184.

Baron-Cohen S, Leslie AM, Frith U (1985) Does the autistic child have a "theory of mind"? Cognition 21:37-46.

Bates D, Maechler M, Bolker B (2013) lme4: Linear mixed-effects models using S4 classes. R package version 0.999999-0. 2012. URL: http://CRAN R-project org/package= lme4.

Bault N, Pelloux B, Fahrenfort JJ, Ridderinkhof KR, van Winden F (2015) Neural dynamics of social tie formation in economic decision-making. Social cognitive and affective neuroscience 10:877-884.

Bellesi G, Vyas K, Jameel L, Channon S (2018) Moral reasoning about everyday situations in adults with autism spectrum disorder. Research in Autism Spectrum Disorders 52:1-11.

Blakemore, Sarah-Jayne, Ouden D, Hanneke, Choudhury, Suparna, Frith, Chris (2007) Adolescent development of the neural circuitry for thinking about intentions. Social Cognitive & Affective Neuroscience 2:130-139.

Blakemore S-J (2008) The social brain in adolescence. Nature Reviews Neuroscience 9:267-277.

Blakemore S-J, Mills KL (2014) Is adolescence a sensitive period for sociocultural processing? Annual Review of Psychology 65:187-207.

Buon M, Dupoux E, Jacob P, Chaste P, Leboyer M, Zalla T (2013) The role of causal and intentional judgments in moral reasoning in individuals with high functioning autism. Journal of autism and developmental disorders 43:458-470.

Burnham KP, Anderson DR (2004) Multimodel inference: understanding AIC and BIC in model selection. Sociological methods & research 33:261-304.

Carter RM, Bowling DL, Reeck C, Huettel SA (2012) A distinct role of the temporal-parietal junction in predicting socially guided decisions. Science 337:109-111.

Channon S, Lagnado D, Fitzpatrick S, Drury H, Taylor I (2011) Judgments of cause and blame: Sensitivity to intentionality in Asperger's syndrome. Journal of autism and developmental disorders 41:1534-1542.

Crockett MJ (2016) How Formal Models Can Illuminate Mechanisms of Moral Judgment and Decision Making. Current Directions in Psychological Science 25:85-90.

D'Cruz A-M, Ragozzino ME, Mosconi MW, Shrestha S, Cook EH, Sweeney JA (2013) Reduced behavioral flexibility in autism spectrum disorders. Neuropsychology 27:152-160.

Dempsey E, Moore C, Johnson S, Stewart S, Smith I (2019) Morality in autism spectrum disorder: A systematic review. Development and psychopathology:1-17.

Dumontheil I, Apperly IA, Blakemore S-J (2010) Online usage of theory of mind continues to develop in late adolescence. Developmental Science 13:331-338.

Eisenberg N, Morris AS (2004) Moral cognitions and prosocial responding in adolescence. In: Handbook of Adolescent Psychology, 2nd Edition (Lerner RM, Steinberg L, eds), pp 155-188. New York: Wiley.

JNeurosci Accepted Manuscript

Eklund A, Nichols TE, Knutsson H (2016) Cluster failure: Why fMRI inferences for spatial extent have inflated false-positive rates. Proceedings of the National Academy of Sciences 113:7900-7905.

Fadda R, Parisi M, Ferretti L, Saba G, Foscoliano M, Salvago A, Doneddu G (2016) Exploring the role of Theory of Mind in moral judgment: the case of children with autism spectrum disorder. Frontiers in psychology 7:523.

Fehr E, Schmidt KM (1999) A theory of fairness, competition, and cooperation. Quarterly Journal of Economics:817-868.

Fox J, Weisberg S, Adler D, Bates D, Baud-Bovy G, Ellison S, Firth D, Friendly M, Gorjanc G, Graves S (2016) Package 'car'.

Frith U, Frith C (2011) Reputation Management: In Autism, Generosity Is Its Own Reward. Current Biology 21:R994-995.

Gelman A, Rubin DB (1992) Inference from iterative simulation using multiple sequences. Statistical Science:457-472.

Gelman A, Carlin JB, Stern HS, Rubin DB (2014) Bayesian data analysis: Chapman & Hall/CRC Boca Raton, FL, USA.

Haley KJ, Fessler DMT (2005) Nobody's watching? Subtle cues affect generosity in an anonymous economic game. Evolution and Human Behavior 26:245-256.

Hampton AN, Bossaerts P, O'Doherty JP (2008) Neural correlates of mentalizing-related computations during strategic interactions in humans. Proceedings of the National Academy of Sciences 105:6741-6746.

Hebart MN, Baker CI (2018) Deconstructing multivariate decoding for the study of brain function. Neuroimage 180:4-18.

Hill CA, Suzuki S, Polania R, Moisa M, O'Doherty JP, Ruff CC (2017) A causal account of the brain network computations underlying strategic social behavior. Nature Neuroscience 20:1142.

Hu Y, He L, Zhang L, Wolk T, Dreher JC, Weber B (2018) Spreading inequality: neural computations underlying paying-it-forward reciprocity. Social Cognitive and Affective Neuroscience 13:578-589.

Hutcherson C, Bushong B, Rangel A (2015) A Neurocomputational Model of Altruistic Choice and Its Implications. Neuron 87:451-462.

Izuma K (2012) The social neuroscience of reputation. Neuroscience research 72:283-288.

Izuma K, Saito DN, Sadato N (2008) Processing of social and monetary rewards in the human striatum. Neuron 58:284-294.

Izuma K, Saito DN, Sadato N (2010a) The roles of the medial prefrontal cortex and striatum in reputation processing. Social Neuroscience 5:133-147.

Izuma K, Saito DN, Sadato N (2010b) Processing of the incentive for social approval in the ventral striatum during charitable donation. Journal of Cognitive Neuroscience 22:621-631.

Izuma K, Matsumoto K, Camerer CF, Adolphs R (2011) Insensitivity to social reputation in autism. Proceedings of the National Academy of Sciences 108:17302-17307.

Kana RK, Keller TA, Cherkassky VL, Minshew NJ, Just MA (2009) Atypical frontal-posterior synchronization of Theory of Mind regions in autism during mental state attribution. Social Neuroscience 4:135-152.

Kilford EJ, Garrett E, Blakemore SJ (2016) The Development of Social Cognition in Adolescence: An Integrated Perspective. Neuroence & Biobehavioral Reviews:106-120.

JNeurosci Accepted Manuscript

Konovalov A, Hu J, Ruff CC (2018) Neurocomputational approaches to social behavior. Current Opinion in Psychology.

Koster-Hale J, Saxe R, Dungan J, Young LL (2013) Decoding moral judgments from neural representations of intentions. Proceedings of the National Academy of Sciences 110:5648-5653.

Kriegeskorte N, Mur M, Bandettini PA (2008) Representational similarity analysis-connecting the branches of systems neuroscience. Frontiers in Systems Neuroscience 2:4.

Lombardo MV, Chakrabarti B, Bullmore ET, Baron-Cohen S, Consortium MA (2011) Specialization of right temporo-parietal junction for mentalizing and its relation to social impairments in autism. Neuroimage 56:1832-1838.

Lopez-Persem A, Rigoux L, Bourgeois-Gironde S, Daunizeau J, Pessiglione M (2017) Choose, rate or squeeze: Comparison of economic value functions elicited by different behavioral tasks. PLoS computational biology 13:e1005848.

Luke SG (2017) Evaluating significance in linear mixed-effects models in R. Behavior Research Methods 49:1494-1502.

Makin TR, Xivry JJOD (2019) Ten common statistical mistakes to watch out for when writing or reviewing a manuscript. Elife Sciences 8:e48175.

Margoni F, Surian L (2016) Mental state understanding and moral judgment in children with autistic spectrum disorder. Frontiers in psychology 7:1478.

Mills KL, Franois L, Clasen LS, Giedd JN, Sarah-Jayne B (2014) Developmental changes in the structure of the social brain in late childhood and adolescence. Social Cognitive and Affective Neuroscience 9:123-131.

Moran JM, Young LL, Saxe R, Lee SM, O'Young D, Mavros PL, Gabrieli JD (2011) Impaired theory of mind for moral judgment in high-functioning autism. Proceedings of the National Academy of Sciences 108:2688-2692.

Morishima Y, Schunk D, Bruhin A, Ruff CC, Fehr E (2012) Linking brain structure and activation in temporoparietal junction to explain the neurobiology of human altruism. Neuron 75:73-79.

Norman KA, Polyn SM, Detre GJ, Haxby JV (2006) Beyond mind-reading: multi-voxel pattern analysis of fMRI data. Trends in cognitive sciences 10:424-430.

Obeso I, Moisa M, Ruff CC, Dreher J-C (2018) A causal role for right temporo-parietal junction in signaling moral conflict. eLife 7:e40671.

Padilla-Walker LM, Carlo G, Memmott-Elison MK (2018) Longitudinal Change in Adolescents' Prosocial Behavior Toward Strangers, Friends, and Family. Journal of Research on Adolescence.

Pantelis PC, Byrge L, Tyszka JM, Adolphs R, Kennedy DP (2015) A specific hypoactivation of right temporo-parietal junction/posterior superior temporal sulcus in response to socially awkward situations in autism. Social cognitive and affective neuroscience 10:1348-1356.

Popal HS, Olson IR, Wang Y (2020) A Guide to Representational Similarity Analysis for Social Neuroscience. Social Cognitive and Affective Neuroscience.

Qu C, Météreau E, Butera L, Villeval MC, Dreher J-C (2019) Neurocomputational mechanisms at play when weighing concerns for extrinsic rewards, moral values, and social image. PLOS Biology 17:e3000283.

Qu C, Hu Y, Tang Z, Derrington E, Dreher JC (2020) Neurocomputational mechanisms underlying immoral decisions benefiting self or others. Social Cognitive and Affective Neuroscience nsaa029.

JNeurosci Accepted Manuscript

R Core Team (2014) R: A language and environment for statistical computing. In.

Salvano-Pardieu V, Blanc R, Combalbert N, Pierratte A, Manktelow K, Maintier C, Lepeltier S, Gimenes G, Barthelemy C, Fontaine R (2016) Judgment of blame in teenagers with Asperger's syndrome. Thinking & Reasoning 22:251-273.

Schaafsma SM, Pfaff DW, Spunt RP, Adolphs R (2014) Deconstructing and reconstructing theory of mind. Trends in Cognitive Sciences 19:65-72.

Schaller UM, Biscaldi M, Fangmeier T, van Elst LT, Rauh R (2019) Intuitive Moral Reasoning in High-Functioning Autism Spectrum Disorder: A Matter of Social Schemas? Journal of autism and developmental disorders 49:1807-1824.

Schurz M, Radua J, Aichhorn M, Richlan F, Perner J (2014) Fractionating theory of mind: A meta-analysis of functional brain imaging studies. Neuroscience & Biobehavioral Reviews 42:9-34.

Stan Development Team (2016) Stan: A C++ library for probability and sampling.

Strombach T, Weber B, Hangebrauk Z, Kenning P, Karipidis II, Tobler PN, Kalenscher T (2015) Social discounting involves modulation of neural value signals by temporoparietal junction. Proceedings of the National Academy of Sciences 112:1619-1624.

Tusche A, Böckler A, Kanske P, Trautwein F-M, Singer T (2016) Decoding the Charitable Brain: Empathy, Perspective Taking, and Attention Shifts Differentially Predict Altruistic Giving. The Journal of Neuroscience 36:4719-4732.

Watanabe T, Lawson RP, Walldén YSE, Rees G (2019) A neuroanatomical substrate linking perceptual stability to cognitive rigidity in autism. The Journal of Neuroence:2831-2818.

Wickham H (2016) ggplot2: elegant graphics for data analysis.

Wolf LK, Bazargani N, Kilford EJ, Dumontheil I, Blakemore SJ (2015) The audience effect in adolescence depends on who's looking over your shoulder. Journal of Adolescence 43:5-14.

Young L, Cushman F, Hauser M, Saxe R (2007) The neural basis of the interaction between theory of mind and moral judgment. Proceedings of the National Academy of Sciences 104:8235-8240.

Young L, Camprodon JA, Hauser M, Pascual-Leone A, Saxe R (2010) Disruption of the right temporoparietal junction with transcranial magnetic stimulation reduces the role of beliefs in moral judgments. Proceedings of the National Academy of Sciences 107:6753-6758.

JNeurosci Accepted Manuscript

Figures

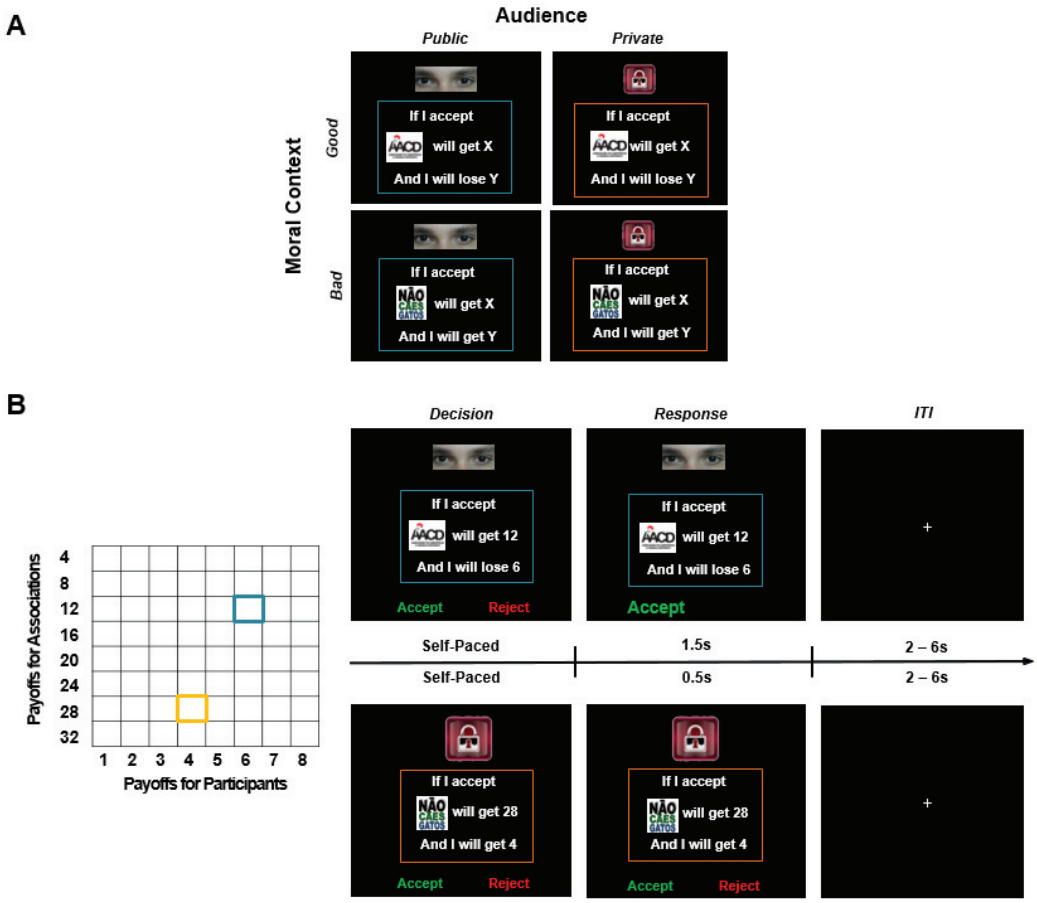

Figure 1. Illustration of Experimental Design and Trial Procedure. (A) We employed a 2 × 2 within-subject design by independently manipulating Audience (Private or Public) and Moral Context (Good or Bad), which yielded four experimental conditions (i.e., $\text{Public}_{\text{Good}}$, $\text{Public}_{\text{Bad}}$, $\text{Private}_{\text{Good}}$, and $\text{Private}_{\text{Bad}}$). The Public condition was indicated by the picture of "eyes", and the Private condition was indicated by the picture of a "lock". The Good context involved a trade-off between personal losses and benefits for a charity, whereas in the Bad context participants traded personal benefits against benefits for a morally-bad cause. (B) Monetary payoffs (in

JNeurosci Accepted Manuscript

Brazilian Real) for participants (8 levels: from 1 to 8, in steps of 1) and the association (8 levels: from 4 to 32, in steps of 4) were orthogonally varied, yielding 64 unique offers for each condition. In the example trial (one for the $Public_{Good}$ and the other for the $Private_{Bad}$ condition), participants were presented with an offer and decided whether to accept or reject the offer with no time limit. If they accepted the offer, both parties involved (i.e., the participant and the association) might undergo the financial consequences as proposed. If they rejected the offer, neither party would profit. In the Private condition, once a response was made, the screen was unchanged for 0.5s to keep the chosen option private. In the Public condition, the chosen option was highlighted with a larger font and the non-chosen option disappeared, this lasted slightly longer (1.5s) to further emphasize the presence of a witness. Each trial was ended with an inter-trial interval (ITI) showing a jittered fixation (2.5 ~ 6.5s).

JNeurosci Accepted Manuscript

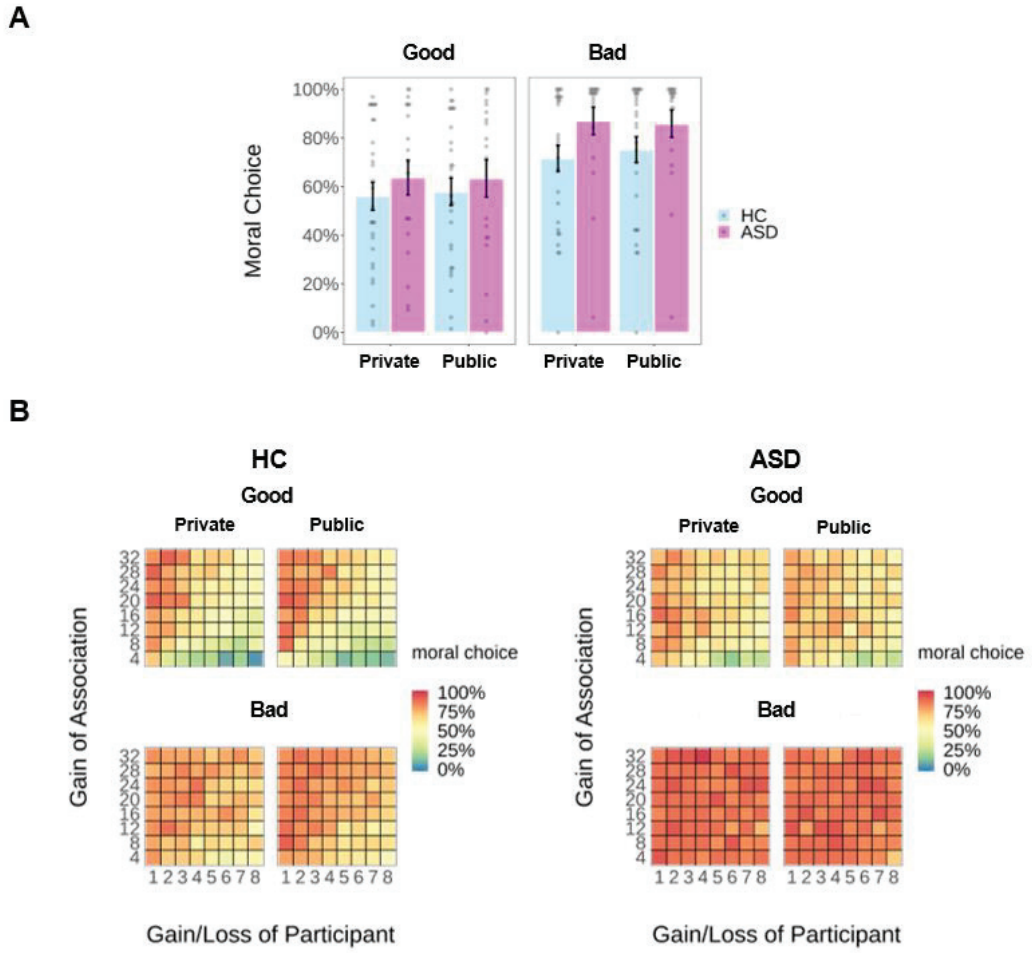

Figure 2. Results of choice behavior. (A) Rate of choosing the moral option as a function of group (ASD or HC), reputation (Private or Public), and context (Good or Bad). (B) Heat map of the mean proportion (%) of moral choices as a function of payoffs (monetary units, MU) for participants and for associations in each experimental condition for each group. Each dot represents the data of a single participant. Error bars represent the SEM; Abbreviation: HC: healthy control, ASD: autism spectrum disorder.

JNeurosci Accepted Manuscript

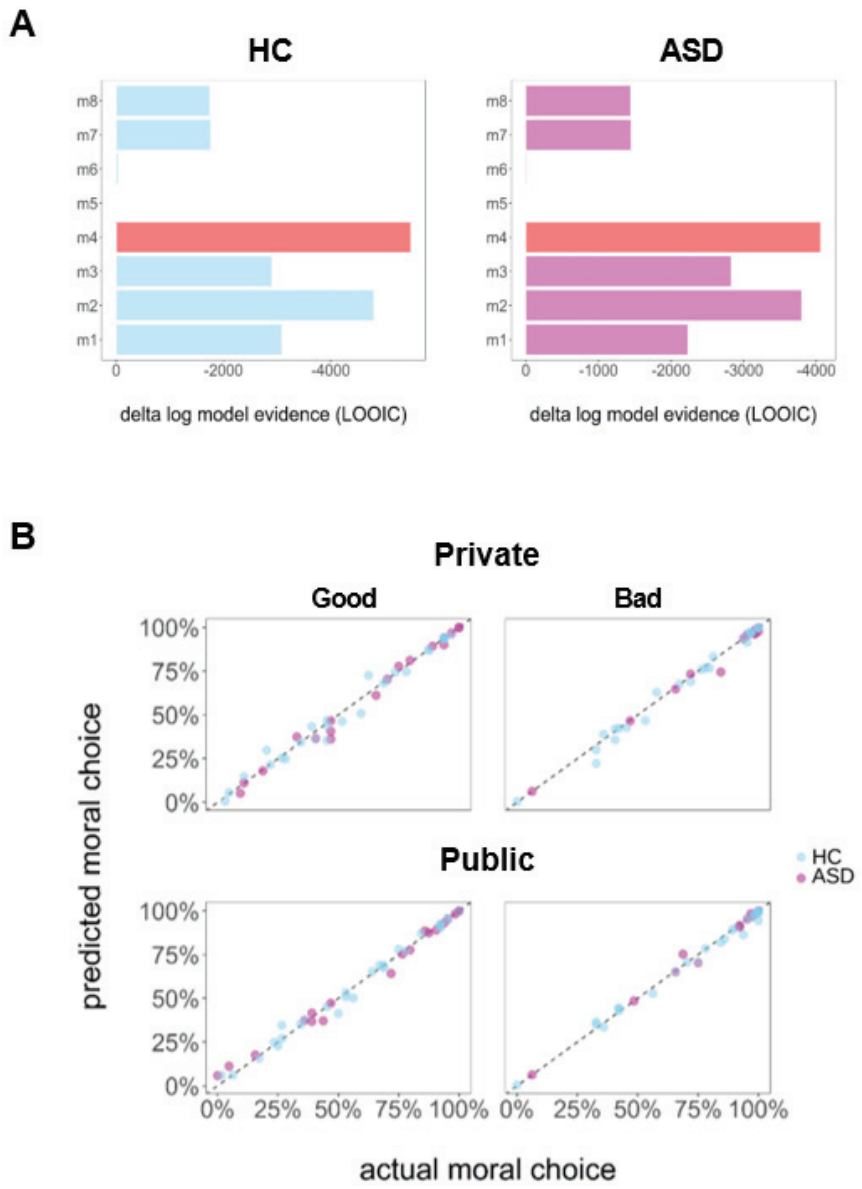

Figure 3. Model comparison and validation. (A) Bayesian model evidence. Model evidence (relative to the model with the worst accuracy of out-of-sample prediction, i.e., model 5), clearly favors model 4 (m4). Lower (i.e., more negative) leave-one-out information criterion (LOOIC) scores indicate a better model. (B) Posterior predictive check of the winning model. Each dot

JNeurosci Accepted Manuscript

represents the data of a single participant. For each participant, we calculated the mean of the predicted proportion of moral choice (%; y axis) by averaging moral choices generated using the whole posterior distribution of estimated parameters specific to that participant based on the winning model. Regardless of experimental conditions, these dots almost fell on the diagonal, indicating that the winning model captured the actual behaviors of all participants in this task. Abbreviation: HC: healthy control, ASD: autism spectrum disorder.

JNeurosci Accepted Manuscript

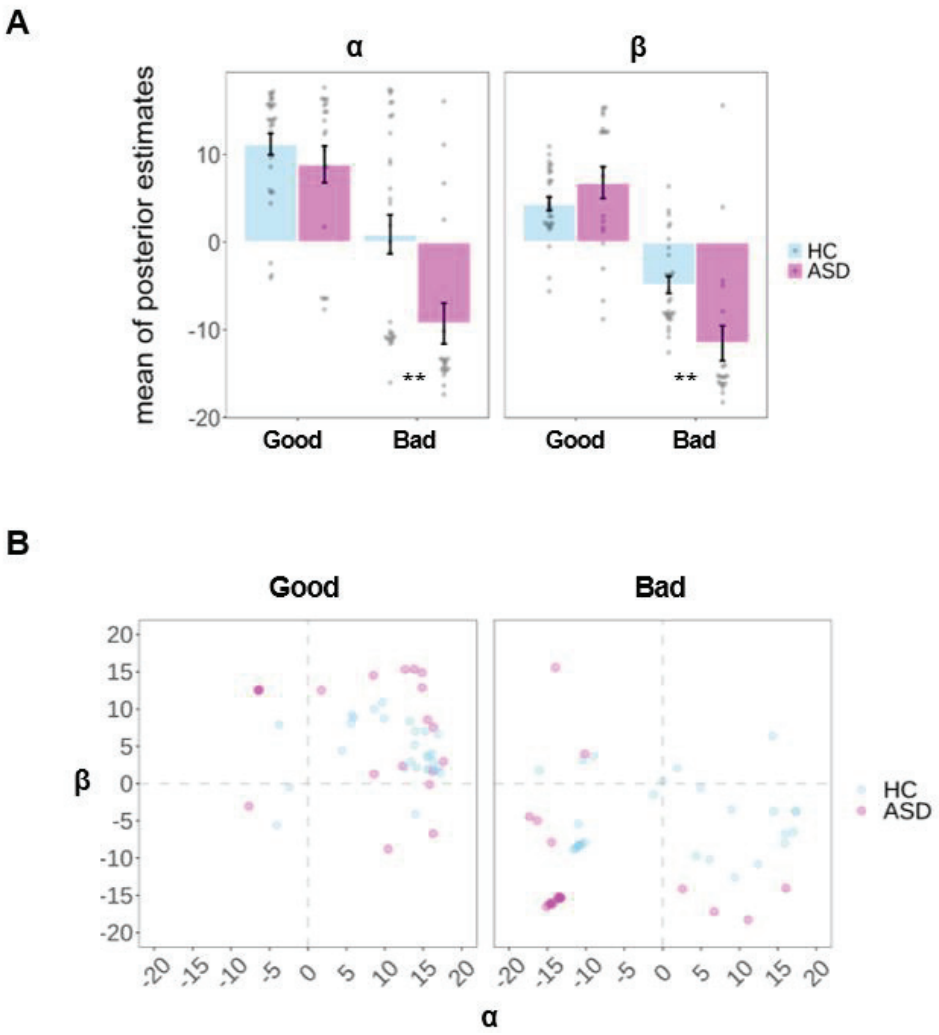

Figure 4. Results of parameter estimates. (A) Group-level mean of individual-level posterior mean of α and β across moral contexts (good or bad) derived from the winning model. (B) Scatter plot of individual-level posterior mean of α and β across moral contexts (Good or Bad) in each group**.** Each dot represents the data of a single participant. Error bars represent the SEM; significance: **p < 0.01, after controlling for the age difference between groups. Abbreviation: HC: healthy control, ASD: autism spectrum disorder.

JNeurosci Accepted Manuscript

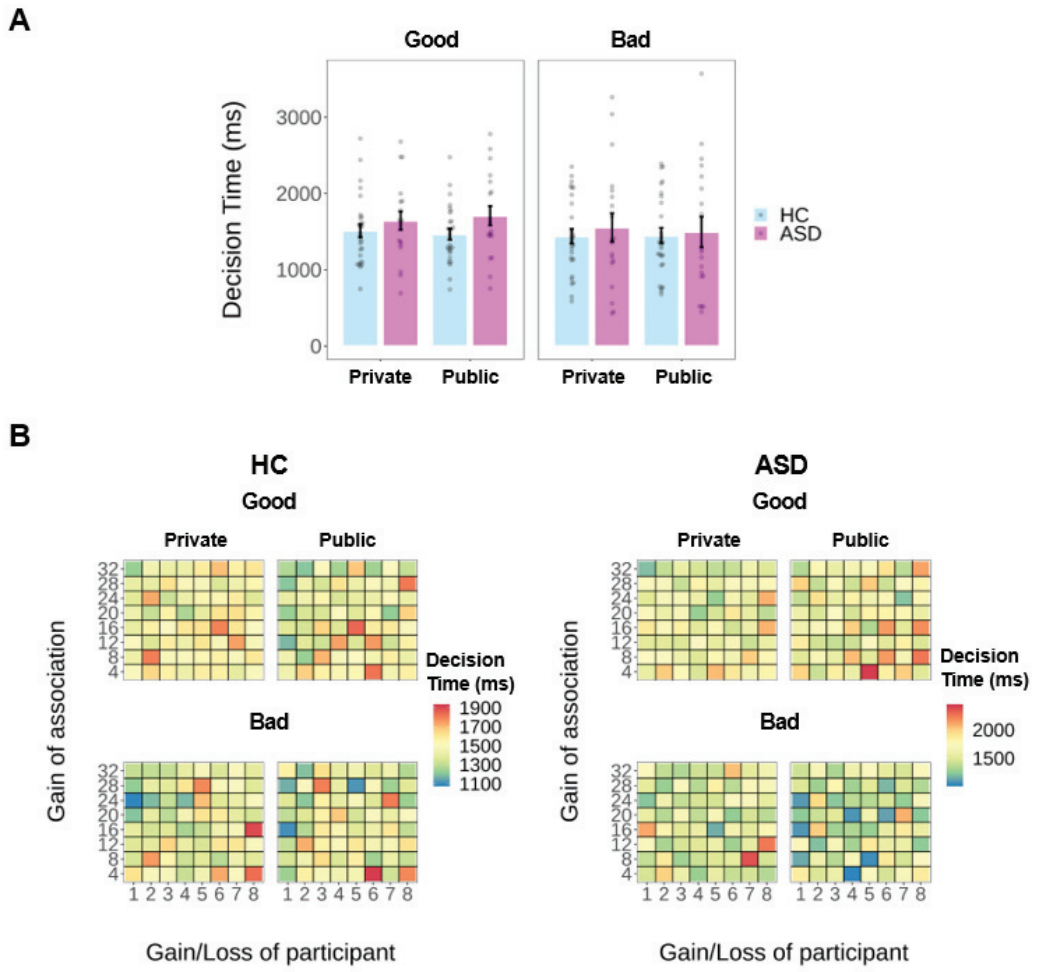

Figure 5. Results of decision time (in ms). (A) Bar plot of the mean decision time as a function of group (ASD or HC), reputation (Private or Public), and context (Good or Bad). (B) Heat map of the mean decision time regardless of specific choices as a function of payoffs (monetary units, MU) for participants and for associations in each experimental condition of each group. Abbreviation: HC: healthy control, ASD: autism spectrum disorder.

JNeurosci Accepted Manuscript

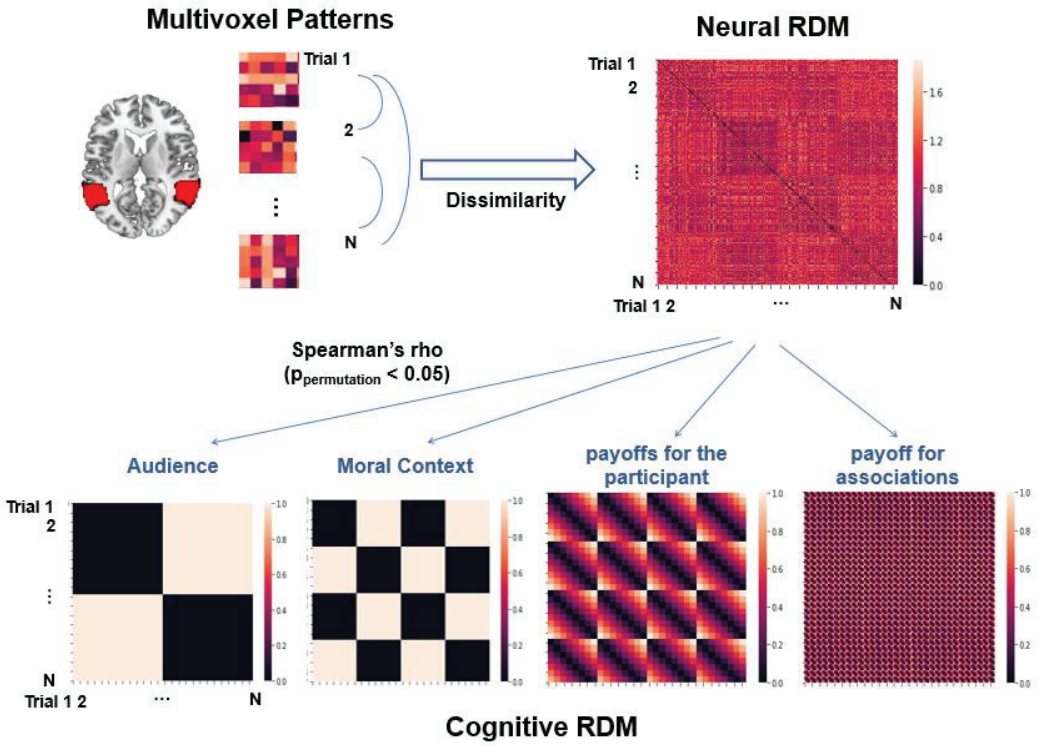

Figure 6. Illustration of within-subject representational similarity analyses (RSA). For each individual, we first constructed a neural RDM measuring the correlational distances of multi-voxel patterns of the decision-relevant neural activities within either left or right TPJ between each pair of valid trials respectively. Next, we constructed four cognitive RDMs by calculating the Euclidean distances between each pair of valid trials with respect to the following information: 1) Audience (i.e., social reputation; Private or Public), 2) Moral Context (i.e., Good or Bad), 3) payoffs for the participant, and 4) payoffs for associations. Notably, we sorted all trials according to the order of Audience, Moral Context, payoff for the participant, and payoff for associations to guarantee the information contained by both the neural and cognitive RDMs was matched with each other. Then we performed the Spearman rank-ordered correlation between

the neural and the cognitive RDMs. Finally, an independent two-sample permutation-based T-test was conducted to compare the between-group difference on the z-transformed Spearman's rho. Abbreviations: RDM: representational dissimilarity matrix.

JNeurosci Accepted Manuscript

JNeurosci Accepted Manuscript

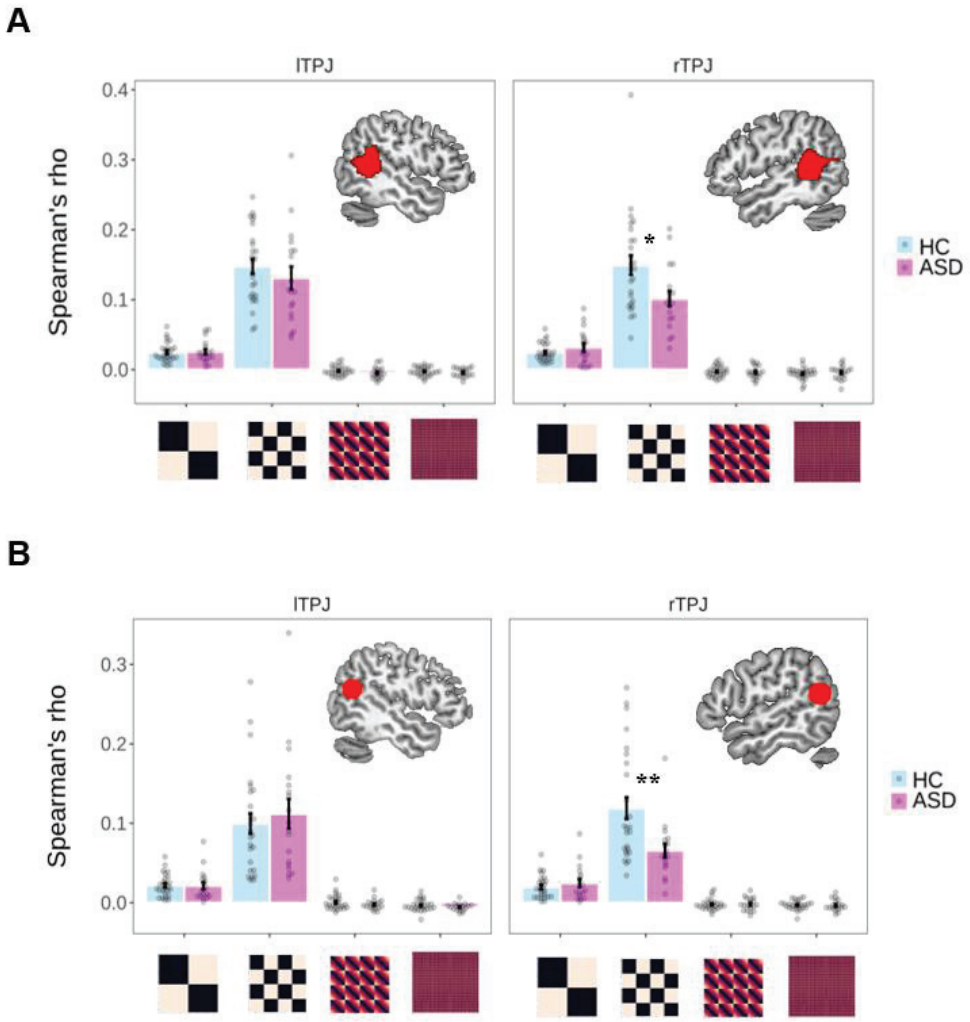

Figure 7. Within-subject RSA results using (A) the Parcellation-Based ROI and (B) the Coordinate-Based ROI of TPJ. For each participant, we only adopted valid trials (see Methods for details) in these analyses. Each dot represents the data of a single participant. Error bars represent the SEM; significance: *$p_{permutation} < 0.05$, **$p_{permutation} < 0.01$, after controlling for the age difference. Abbreviation: RSA: representational similarity analysis; TPJ: temporoparietal junction; HC: healthy control, ASD: autism spectrum disorder.

JNeurosci Accepted Manuscript

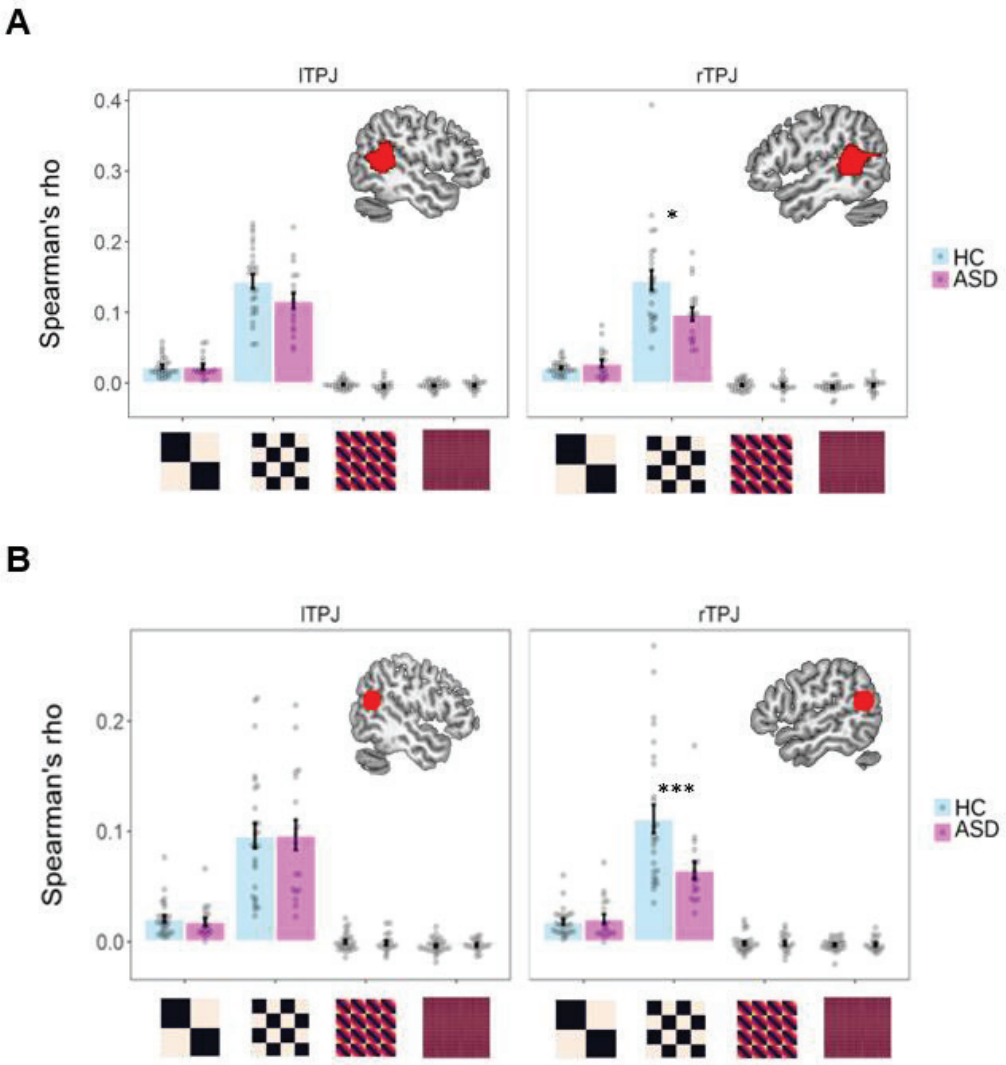

Figure 8. Robustness check of within-subject RSA results using (A) the Parcellation-Based ROI and (B) the Coordinate-Based ROI of TPJ. For each participant, we adopted all 256 trials in these analyses. Each dot represents the data of a single participant. Error bars represent the SEM; significance: *$p_{permutation} < 0.05$, ***$p_{permutation} < 0.001$, after controlling for the age difference. Abbreviation: RSA: representational similarity analysis; TPJ: temporoparietal junction; HC: healthy control, ASD: autism spectrum disorder.

JNeurosci Accepted Manuscript

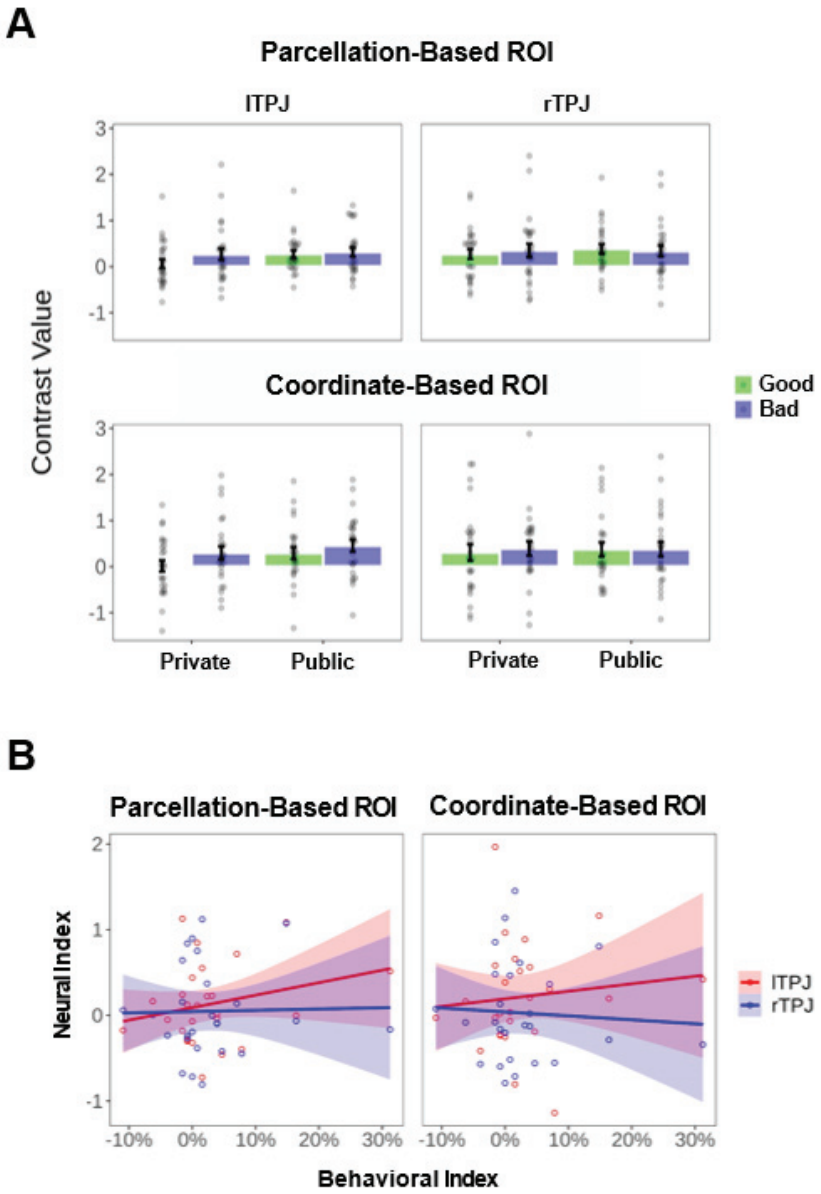

Figure 9 Univariate results of TPJ in healthy controls. (A) Bar plot of TPJ signals. For visualization, we extracted the mean activity (contrast value) of lTPJ and rTPJ from the parcellation-based or coordinate-based mask as a function of reputation (Private or Public), and context (Good or Bad). Each dot represents the data of a single participant. Error bars represent

JNeurosci Accepted Manuscript

the SEM. **(B) Relationship between neural audience effect in TPJ and behavioral audience effect across individuals.** Each dot represents the data of a single participant. Each line represents the linear fit. Shaded areas represent the 95% confidence interval. Abbreviation: ROI: region of interest; TPJ: temporoparietal junction.

JNeurosci Accepted Manuscript

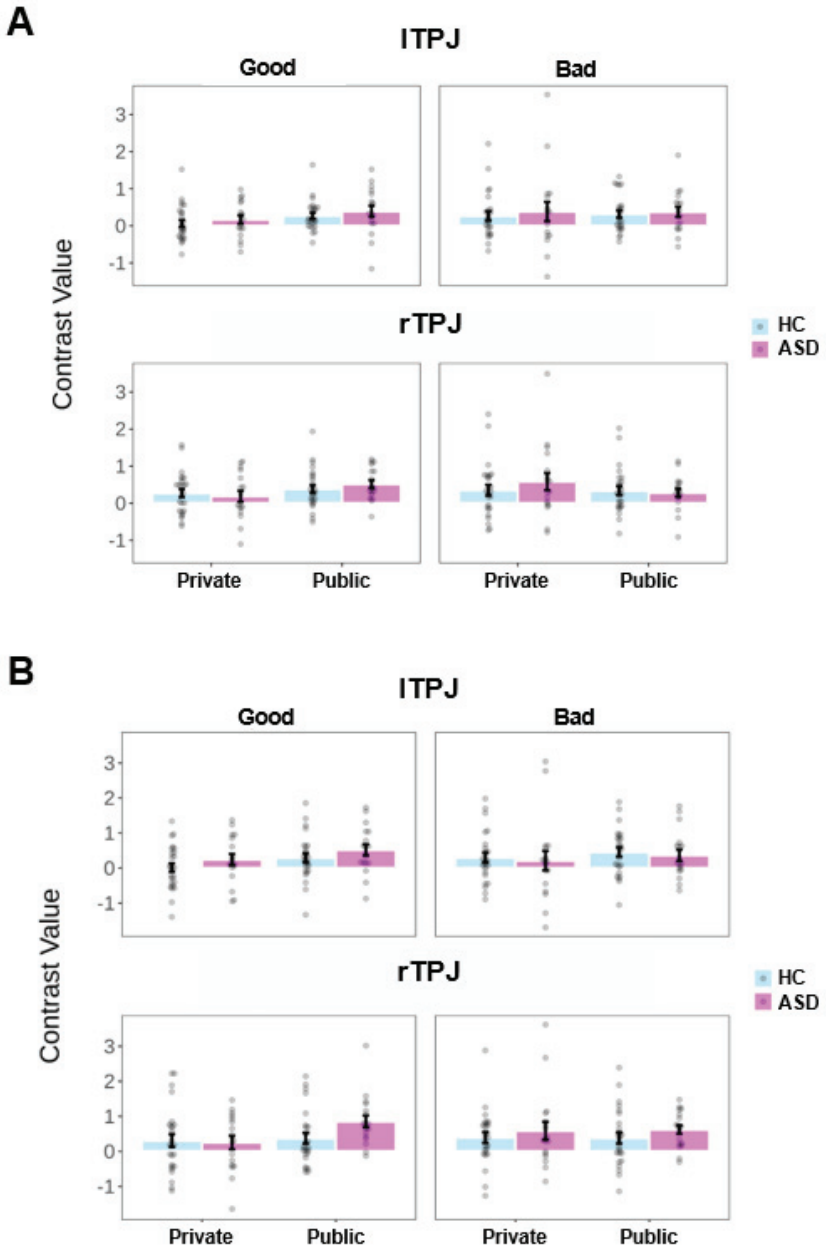

Figure 10 Univariate results of TPJ in HC and ASD group using (A) the parcellation-based mask and (B) the coordinate-based mask. For visualization, we extracted the mean activity

JNeurosci Accepted Manuscript

(contrast value) of lTPJ and rTPJ from the corresponding masks as a function of group (ASD or HC), reputation (Private or Public), and context (Good or Bad). Each dot represents the data of a single participant. Error bars represent the SEM.

JNeurosci Accepted Manuscript

1005 ## Tables

1006 **Table 1 Summary of clinical measures in two groups**

	ASD	HC
IQ: total[a]	100.0 ± 10.0	105.0 ± 8.9
IQ: verbal[a]	103.2 ± 9.9	103.2 ± 9.2
IQ: execution[a]	106.7 ± 12.4	106.7 ± 11.5
ADI-R: social	21.0 ± 5.2	
ADI-R: communication	14.0 ± 4.5	
ADI-R: repetitive	6.7 ± 1.7	

1007

1008 Note: [a] IQ was measured by Wechsler Intelligence Scale for Children (WISC); Data of 3 HC were
1009 missing. Abbreviations: IQ: intelligence quotient, ADI: autism diagnostic interview; HC: healthy
1010 control, ASD: autism spectrum disorder.

JNeurosci Accepted Manuscript

1011 **Table 2 Results of mixed-effect logistic regressions predicting moral choices**

	All	Good	Bad	Bad: Private	Bad: Public
	b (SE)	*b* (SE)	*b* (SE)	*b* (SE)	*b* (SE)
Intercept	0.63 (0.39)	0.54 (0.53)	2.64** (0.81)	2.57** (0.84)	3.26*** (0.88)
Group	0.86 (0.64)	1.31 (0.86)	3.41* (1.42)	4.16** (1.53)	2.32 (1.44)
Audience	0.11 (0.08)	0.15 (0.10)	0.27** (0.10)		
Moral context	0.95*** (0.08)				
Group × Audience	-0.17 (0.13)	-0.23 (0.16)	-0.44* (0.22)		
Group × Moral context	0.89*** (0.15)				
Audience × Moral context	0.09 (0.12)				
Group × Audience × Moral context	-0.11 (0.21)				
Payoff for oneself[a,b]		-0.99*** (0.04)	-0.46*** (0.05)	-0.39*** (0.07)	-0.56*** (0.07)
Payoff for association[a,b]		0.83*** (0.04)	0.33*** (0.05)	0.34*** (0.06)	0.35*** (0.07)
Age[a]	0.19 (0.32)	0.50 (0.43)	0.26 (0.70)	0.23 (0.70)	0.12 (0.73)
AIC	10501.0	4340.7	3148.7	1649.7	1551.1
BIC	10574.8	4394.1	3202.2	1685.6	1587.1
N (Observation)	11823	5912	5911	2948	2963
N (Participant)	47	47	47	47	47

1012

1013 Note: [a] We standardized these variables for the analyses.

1014 [b] These variables were added as covariates only when the regressor "Association" (and its interaction)

1015 was not in the regression model, as the regressor "payoff for oneself" qualitatively co-varied with

1016 "Association", which might cause the collinear issue.

1017 Reference levels were set as follows: Group = healthy controls (HC), Audience = Private, Moral Context =

1018 Good. Table also shows goodness-of-fit statistics: AIC = Akaike Information Criterion, BIC = Bayesian

1019 Information Criterion. Significance: $^{*}p < 0.05$, $^{**}p < 0.01$, $^{***}p < 0.001$.

JNeurosci Accepted Manuscript

1020 **Table 3 Results of mixed-effect logistic regressions predicting log-transformed decision**

	All	Good	Good: Private	Good: Public	Bad
	b (SE)	*b* (SE)	*b* (SE)	*b* (SE)	*b* (SE)
Intercept	7.22*** (0.07)	7.19*** (0.06)	7.19*** (0.06)	7.18*** (0.06)	7.19*** (0.10)
Group	0.07	0.04	0.04	0.09	-0.04

1021 **time (in ms)**

JNeurosci Accepted Manuscript

	(0.11)	(0.09)	(0.10)	(0.09)	(0.14)
Audience	-0.01	-0.02			0.01
	(0.02)	(0.01)			(0.01)
Moral context	-0.08***				
	(0.02)				
Group × Audience	0.04	0.04*			-0.04†
	(0.02)	(0.02)			(0.02)
Group × Moral context	-0.13***				
	(0.02)				
Audience × Moral context	0.02				
	(0.02)				
Group × Audience × Moral context	-0.08*				
	(0.03)				
Decision	-0.02†	0.04*	0.05*	0.03	-0.10***
	(0.01)	(0.01)	(0.02)	(0.02)	(0.02)
Payoff for oneself[a,b]		0.03***	0.02*	0.04***	0.02**
		(0.01)	(0.01)	(0.01)	(0.01)
Payoff for association[a,b]		-0.03***	-0.03***	-0.03***	-0.01*
		(0.01)	(0.01)	(0.01)	(0.006)
Age[a]	0.03	-0.001	-0.01	0.005	0.05
	(0.05)	(0.05)	(0.05)	(0.05)	(0.07)
AIC	15114.8	6095.5	3074.3	3058.6	7203.8
BIC	15203.4	6162.4	3122.2	3106.5	7270.6
N (Observation)	11823	5912	2952	2960	5911
N (Participant)	47	47	47	47	47

Note: [a] We standardized these variables for the analyses.

[b] These variables were added as covariates only when the regressor "Association" (and its interaction) was not in the regression model, as the regressor "payoff for oneself" qualitatively co-varied with "Association", which might cause the collinear issue.

Reference levels were set as follows: Group = NC, Audience = private, Association = good cause (charity). Table also shows goodness-of-fit statistics: AIC = Akaike Information Criterion, BIC = Bayesian Information Criterion. Significance: $^{\dagger}p < 0.06$, $^{*}p < 0.05$, $^{**}p < 0.01$, $^{***}p < 0.001$.

JNeurosci Accepted Manuscript

1030 **Table 4 Within-subject RSA results in TPJ using valid trials[a]**

			Spearman's rho (mean ± SD)			
			ASD	HC	$p_{permutation}$	$p_{permutation}$[c]
Neurosynth	lTPJ	Audience	0.026 ± 0.016***	0.025 ± 0.014***	0.848	0.493
		Moral context	0.131 ± 0.069***	0.148 ± 0.054***	0.403	0.493
		Payoff for oneself	-0.005 ± 0.008	-0.002 ± 0.007	0.174	0.271
		Payoff for association	-0.004 ± 0.006	-0.003 ± 0.006	0.413	0.447
	rTPJ	Audience	0.032 ± 0.025***	0.024 ± 0.013***	0.201	0.163
		Moral context	**0.101 ± 0.047*** **	**0.150 ± 0.071*** **	**0.013**	**0.018**
		Payoff for oneself	-0.004 ± 0.009	-0.003 ± 0.007	0.723	0.311
		Payoff for association	-0.004 ± 0.010	-0.006 ± 0.009	0.578	0.995
Meta-Analysis[b]	lTPJ	Audience	0.021 ± 0.019***	0.022 ± 0.014***	0.912	0.931
		Moral context	0.112 ± 0.079***	0.100 ± 0.065***	0.566	0.551
		Payoff for oneself	-0.002 ± 0.007	0.0005 ± 0.009	0.304	0.472
		Payoff for association	-0.005 ± 0.005	-0.003 ± 0.007	0.308	0.262
	rTPJ	Audience	0.025 ± 0.022***	0.020 ± 0.014***	0.383	0.230
		Moral context	**0.066 ± 0.036*** **	**0.119 ± 0.070*** **	**0.006**	**0.002**
		Payoff for oneself	-0.002 ± 0.008	-0.002 ± 0.007	0.900	0.685
		Payoff for association	-0.003 ± 0.007	-0.003 ± 0.006	0.924	0.400

1031

1032 Note: [a]We excluded trials that did not reach the behavioral criterion (i.e., those with a decision time [DT]
1033 shorter than 200ms or longer than mean ± 3*SD of that individual) or fMRI criterion (all trials in a run with
1034 an excessive head motion: ASD: > 5mm; HC: > 3mm). [b] These masks were spheres with a radius of
1035 10mm centering on the MNI coordinates based on a recent meta-analysis involving the mentalizing
1036 process (peak MNI coordinates: left TPJ/pSTS: -53/-59/20; right TPJ/pSTS: 56/-56/18).
1037 [c] We added the standardized age as the covariates to the regression, using the lmPerm package.
1038 *** These effects are significantly higher than 0 (i.e., one-sample T-test with 5000 permutations; $p_{permutation}$
1039 < 0.001).

JNeurosci Accepted Manuscript

Abbreviations: l: left, r: right, TPJ: temporoparietal junction; ASD: autism spectrum disorder, HC: healthy control.

JNeurosci Accepted Manuscript

Table 5 Within-subject RSA results in TPJ using all 256 trials

			Spearman's rho (mean ± SD)			
			ASD	HC	$p_{permutation}$	$p_{permutation}$[b]
Neurosynth	lTPJ	Audience	0.023 ± 0.016***	0.023 ± 0.014***	0.967	0.538
		Moral context	0.117 ± 0.047***	0.144 ± 0.050***	0.063	0.094
		Payoff for oneself	-0.004 ± 0.009	-0.002 ± 0.006	0.299	0.358
		Payoff for association	-0.003 ± 0.006	-0.003 ± 0.006	0.932	0.919
	rTPJ	Audience	0.028 ± 0.022***	0.022 ± 0.010***	0.203	0.169
		Moral context	**0.098 ± 0.040*** **	**0.146 ± 0.070*** **	**0.009**	**0.027**
		Payoff for oneself	-0.003 ± 0.009	-0.003 ± 0.007	0.854	0.387
		Payoff for association	-0.003 ± 0.009	-0.005 ± 0.008	0.386	0.667
Meta-Analysis[a]	lTPJ	Audience	0.018 ± 0.015***	0.021 ± 0.016***	0.579	0.850
		Moral context	0.097 ± 0.058***	0.096 ± 0.058***	0.972	0.914
		Payoff for oneself	-0.001 ± 0.008	-0.00004 ± 0.008	0.721	0.745
		Payoff for association	-0.003 ± 0.005	-0.004 ± 0.007	0.775	0.871
	rTPJ	Audience	0.021 ± 0.019***	0.018 ± 0.013***	0.613	0.451
		Moral context	**0.067 ± 0.034*** **	**0.111 ± 0.064*** **	**0.006**	**< 0.001**
		Payoff for oneself	-0.001 ± 0.008	-0.001 ± 0.008	0.990	0.528
		Payoff for association	-0.002 ± 0.006	-0.003 ± 0.006	0.796	0.689

Note: *Post-hoc* 2 (group) × 4 (cognitive RDM) mixed ANOVA on the Fisher r-to-z transformed Spearman's rho revealed a strong interaction between group and cognitive RDM only in rTPJ regardless of the way we defined the ROI (the parcellation-based ROI: $F(3,126) = 6.59$, $p < 0.001$; the coordinate-based ROI: $F(3,126) = 7.37$, $p < 0.001$), which was not true in lTPJ (the parcellation-based ROI: $F(3,126) = 3.00$, $p = 0.033$; the coordinate-based ROI: $F(3,126) = 0.03$, $p = 0.994$) after controlling for the age difference, which further confirmed that the specific between-group effect in representing information of Moral Context was unique in rTPJ.

JNeurosci Accepted Manuscript

[a] These masks were spheres with a radius of 10mm centering on the MNI coordinates based on a recent meta-analysis involving the mentalizing process (peak MNI coordinates: left TPJ/pSTS: -53/-59/20; right TPJ/pSTS: 56/-56/18).

[b] We added the standardized age as the covariates to the regression, using the lmPerm package.

*** These effects are significantly higher than 0 (i.e., one-sample T-test with 5000 permutations; $p_{permutation} < 0.001$).

Abbreviations: l: left, r: right, TPJ: temporoparietal junction; ASD: autism spectrum disorder, HC: healthy control.

JNeurosci Accepted Manuscript

1059 **Table 6 Supplementary univariate GLM results**[a]

Brain Region	Hemisphere	Cluster Size	MNI			BA	T-value	p(cl-FWE)
			x	y	z			
ASD								
Public > Private								
Cingulate Gyrus/ Corpus Callosum	L	96	-16	8	30		4.99	0.162
HC > ASD								
Private > Public								
Cingulate Gyrus/ Corpus Callosum	L	71	-10	2	30		4.33	0.371
Good > Bad								
Prec/SOG	L	95	-18	-58	32	7	4.84	0.229
IPL/PoCG	L	56	-38	-32	44	40	3.59	0.525

1060

1061 Note: [a]We excluded trials that did not reach the behavioral criterion (i.e., those with a decision time
1062 shorter than 200ms or longer than mean ± 3*SD of that individual) or fMRI criterion (all trials in a run with
1063 an excessive headmotion).

1064 Regions shown here met an uncorrected voxel-level threshold of $p < 0.001$ with $k = 50$. Coordinates
1065 shown here were based on Montreal Neurological Institute (MNI) coordinate system. Abbreviations: ASD:
1066 autism spectrum disorder, HC: healthy control; L: left, R: right, B: bilateral, BA: Brodmann Area; cl-FWE:
1067 cluster-level Family-Wise Error (corrected); CC: corpus callosum, CG: cingulate gyrus, IPL: inferior
1068 parietal lobule, PoCG: post-central gyrus, Prec: precuneus, SOG: superior occipital gyrus.